Università degli Studi di Cagliari

DOTTORATO DI RICERCA IN

"*Patologia e Tossicologia Ambientale*"

"XXI ciclo"

Settore Scientifico Disciplinare: MED/04

EFFECT OF THE LIGANDS OF THYROID HORMONE RECEPTOR ON NON-ALCOHOLIC FATTY LIVER DISEASE

Presentata da: Marta Anna Kowalik

Coordinatore dottorato: Prof. Amedeo Columbano

Relatore: Prof. Amedeo Columbano

Esame finale a.a 2007-2008

ACKNOWLEDGEMENTS

A few lines are too short to express my deep appreciation and to thank Prof. Amedeo Columbano and Prof. Giovanna Maria Ledda-Columbano for accepting me as their PhD student. I owe them my intellectual development during these three years.

I am deeply grateful to Dr. Julian L. Griffin and Dr. Aalim M. Weljie from the University of Cambridge for providing me with the results of UPLC-QTOF-MS and to Prof. Luigi Atzori who was always willing to help me in understanding them and in gathering the required information for the accomplishment of this thesis.

I wish to sincerely thank Assistant Prof. Gabriella Simbula for her enlightened guidance, assistance, and constructive suggestions during the correction of this dissertation. Her conceptual insights into my thesis work have been invaluable.

Sincere and heartfelt thanks are extended to Assistant Prof. Monica Pibiri and Dr. Vera P. Leoni.

I am also grateful to Dr. Andrea Perra (MD) for his constant help.

I want to thank my laboratory colleagues and wish them all the best for their future careers.

This thesis is dedicated to my grandparents and parents who have always supported and encouraged me to do my best in all matters of life, and to my husband without whom none of this would have even been possible.

CONTENTS

LIST OF ABBREVIATIONS

ADP	adenosine diphosphate
ALT	alanine aminotransferase
AST	aspartate aminotransferase
ATP	adenosine triphosphate
BHMT	betaine:homocysteine methyltransferase
CAR	constitutive androstane receptor
CDP	cytidine diphosphate
CK	choline kinase
CMD	choline-deficient, methionine-restricted
CMP	cytidine monophosphate
COX-2	cyclooxygenase-2
CPT	CDP-choline:DAG cholinephosphotransferase
CTP	cytidine triphosphate
DAG	diacylglycerol
DBD	DNA-binding domain
DENA	diethylnitrosamine
FFA	free fatty acid
FLD	fatty liver disease
FXR	farnesoid X receptor
GGT	γ-glutamyltranspeptidase
GS	gas chromatography
HCC	hepatocellular carcinoma
HL	hepatic lipase
HSL	hormone-sensitive lipase
ICAM	intercellular adhesion molecule
IL-6	interleukin-6
JNK	c-Jun N-terminal kinase
LBD	ligand-binding domain
LC	liquid chromatography

LPL	lipoprotein lipase
LXR	liver X receptor
MAT	methionine adenosyltransferase
methylTHF	5-methyltetrahydrofolate
MS	mass spectrometry
MTHF	5,10-methylene-tetrahydrofolate
MTP	microsomal triglyceride transfer protein
NAFLD	non-alcoholic fatty liver disease
NASH	non-alcoholic steatohepatitis
NF-κB	nuclear factor kappa B
NR	nuclear receptor
PAF	platelet-activating factor
PC	phosphatidylcholine
PCP	phosphatidylcholine:ceramidecholine phosphotransferase
Pcyt1	CTP:phosphocholine cytidyltransferase
PEMT	phosphatidylethanolamine N-methyltransferase
PLA	phospholipase A2
PP	peroxisome proliferator
PPAR	peroxisome proliferator-activated receptor
PXR	pregnane X receptor
ROS	reactive oxygen species
SAH	S-adenosylhomocysteine
SAM	S-adenosylmethionine
SAPK	stress-activated protein kinase
SCPx	sterol carrier protein x
SE	standard error
SREBP-1	sterol regulatory element binding protein-1
STATs	signal transducers and activators of transcription
T3	triiodothyronine
TG	triglyceride
TGF	transforming growth factor
TH	thyroid hormone
THF	tetrahydrofolate

TNF-α	tumour necrosis factor α
TOF	time-of-flight
TR	thyroid hormone receptor
TRE	thyroid response element
TSH	thyroid-stimulating hormone
UPLC	ultra-performance liquid chromatography
VCAM	vascular cell adhesion molecule
VLDL	very low density lipoprotein
8-OH-dG	8-hydroxydeoxyguanosine

PREMESSA

L'epatopatia steatosica non alcolica (non-alcoholic fatty liver disease, NAFLD) si riferisce ad uno spettro di quadri clinici che vanno dalla steatosi semplice alla steatosi con aspetti necro-infiammatori (steatoepatite), alla fibrosi e infine alla cirrosi, e rappresenta una delle più comuni patologie epatiche nei paesi occidentali (Farrell and Larter, 2006). Dai dati scientifici recentemente pubblicati emerge che lo stadio di cirrosi può richiedere un trapianto di fegato ed è associato in maniera rilevante al rischio di sviluppo del carcinoma epatocellulare (hepatocellular carcinoma, HCC) (Jiang and Torok, 2008). E' opportuno mettere in evidenza che la NAFLD è presente non solo negli adulti, ma sono in aumento le diagnosi nei pazienti in età pediatrica. Secondo le previsioni dell'Organizzazione Mondiale della Sanità (World Health Organization, WHO), almeno 2 milioni di persone svilupperanno la cirrosi come conseguenza della steatosi epatica e la NAFLD diventerà la causa principale di trapianti di fegato nei prossimi decenni (Schreuder *et al.*, 2008). Per questo motivo, la steatosi epatica non dovrebbe essere considerata come una condizione innocua, ma piuttosto come un importante fattore di rischio con un potenziale evolutivo verso patologie epatiche più avanzate (den Boer *et al.*, 2004; Bradbury, 2006). Purtroppo, fino ad ora nessun trattamento specifico per i pazienti colpiti dalla NAFLD si è dimostrato completamente efficace (Schreuder *et al.*, 2008).

Negli ultimi anni, una notevole attenzione è stata indirizzata sui recettori nucleari come possibili bersagli di farmaci nella terapia farmacologia (Tobin and Freedman, 2006). Alcuni membri della superfamiglia dei recettori nucleari [p.es. peroxisome proliferator-activated receptors (PPARs), constitutive androstane receptor (CAR), liver X receptor (LXR), farnesoid X receptor (FXR), pregnane X receptor (PXR)] che fungono da fattori trascrizionali, funzionano come sensori intracellulari dei metaboliti del colesterolo, degli acidi grassi e delle molecole lipofiliche con un ruolo fondamentale nell'omeostasi energetica, nel metabolismo lipidico e nell'infiammazione (George and Liddle, 2007). Sino ad oggi, soltanto gli agonisti PPARγ (tiazolidinedioni) e PPARα (clofibrato) sono stati testati in studi pilota su pazienti umani (Laurin *et al.*, 1996; Miyazaki *et al.*, 2002; Neuschwander-Tetri *et al.*, 2003a; Sanyal *et al.*, 2004; Belfort *et al.*, 2006). Tuttavia, la

scoperta di rilevanti effetti collaterali derivanti dall'utilizzo di questa classe di farmaci ha stimolato ulteriori ricerche nel campo dei recettori nucleari mediante l'uso sia di modelli cellulari che animali (George and Liddle, 2007).

I processi correlati al metabolismo dei lipidi e del colesterolo sono influenzati anche dagli ormoni tiroidei, in particolare dalla triiodotironina (T3). Suscita interesse il fatto che l'attività biologica del T3 deriva dall'attivazione dei recettori per gli ormoni tiroidei che appartengono alla suddetta superfamiglia dei recettori nucleari. Il potenziale terapeutico degli agonisti del recettore dell'ormone tiroideo, come gli agenti in grado di ridurre il peso corporeo e i lipidi ematici, è stato a lungo l'obiettivo della ricerca (Moreno *et al.*, 2008). Tuttavia, l'ipotetico effetto del T3 sulla NAFLD rimane ancora largamente inesplorato.

Di conseguenza, ci è sembrato di notevole interesse esaminare quest'ipotesi. Lo scopo di questa tesi, quindi, è stato quello di valutare l'effetto del T3 e di un analogo strutturale del recettore dell'ormone tiroideo sulla steatosi epatica.

INTRODUCTION

The term non-alcoholic fatty liver disease (NAFLD) has been used as a general name for conditions ranging from simple steatosis to steatohepatitis, advanced fibrosis and cirrhosis. NAFLD, present in up to one-third of the general population with a very high prevalence in North and South America, Asia-Pacific (including Australia and New Zealand), the Middle East and Europe, is emerging as one of the most common liver diseases (Farrell and Larter, 2006). Newly published scientific data demonstrate that end-stage NAFLD cirrhosis may require liver transplantation and carries a substantial risk for early hepatocellular carcinoma (HCC) development (Jiang and Torok, 2008). Worryingly, NAFLD is also reported increasingly in paediatric patients. According to the World Health Organization (WHO) predictions, at least two million people will develop cirrhosis due to hepatic steatosis and NAFLD will become the leading indication for liver transplantation in the next decades (Schreuder *et al.*, 2008). In this respect, the awareness and the importance of diagnosing this alarming entity should be emphasized. Furthermore, it becomes evident that hepatic steatosis should not be regarded as an innocuous, benign condition, even in its bland form, but rather as a growing public health concern and an important cause of advanced liver disease (den Boer *et al.*, 2004; Bradbury, 2006). Up till now, no exact treatment strategy for patients suffering from NAFLD has been conclusively proved to be effective (Schreuder *et al.*, 2008).

Recently, considerable interest has been focused on nuclear receptors as attractive drug targets for the management of NAFLD (Tobin and Freedman, 2006). Some members of the large superfamily of nuclear hormone receptors [e.g. peroxisome proliferator-activated receptors (PPARs), constitutive androstane receptor (CAR), liver X receptor (LXR), farnesoid X receptor (FXR), pregnane X receptor (PXR)] which function as ligand-activated transcription factors, are known to act as intracellular sensors for cholesterol metabolites, free fatty acids, and a range of other lipophilic molecules with critical roles in energy homeostasis, lipid metabolism and inflammation (George and Liddle, 2007). To date, only PPARγ (thiazolidinediones: troglitazone, rosiglitazone and pioglitazone) and PPARα (clofibrate) agonists have been investigated in human pilot studies (Laurin *et al.*, 1996; Miyazaki *et al.*, 2002; Neuschwander-Tetri *et al.*, 2003a; Sanyal *et al.*, 2004; Belfort *et al.*, 2006). However, it has been discovered that these drugs have significant side effects, so alternate approaches to nuclear receptor targeting are being explored in animal- or cell-based models (George and Liddle, 2007).

The processes and pathways related to lipid and cholesterol handling are also affected by thyroid hormones (THs), in particular triiodothyronine (T3). Interestingly, biological activity of T3 arises from activation of TH receptors (TRs) which are members of the abovementioned superfamily of nuclear hormone receptors. The therapeutic potential of thyroid hormone receptor agonists as lipid- and weight-lowering agents has long been the focus of research (Moreno *et al.*, 2008). However, the hypothetical effect of T3 on NAFLD remained largely unexplored.

Consequently, it seemed to us particularly noteworthy to broaden this concept and the aim of this dissertation was to examine the influence of T3 and TH structural analog on fatty liver disease.

INTRODUCTION

Lipid flux in the liver and hepatic steatosis

The liver is a central player in the whole body energy homeostasis by its ability to store glucose in the form of glycogen and distribute fuel sources (glucose and lipids) to peripheral tissues. It is also known to be a major regulator of metabolite flow in the body (Reddy and Rao, 2006) and to play a fundamental role in lipid metabolism through (Fig. 1):

- the uptake of fatty acids;
- fatty acid oxidation;
- *de novo* fatty acid synthesis, a key metabolic pathway for energy homeostasis in higher animals;
- assembly and secretion of very low density lipoprotein-triglyceride (VLDL-TG);
- effects of fatty acids on gene expression by controlling the activity or abundance of key transcription factors (den Boer *et al.*, 2004; Jump *et al.*, 2005).

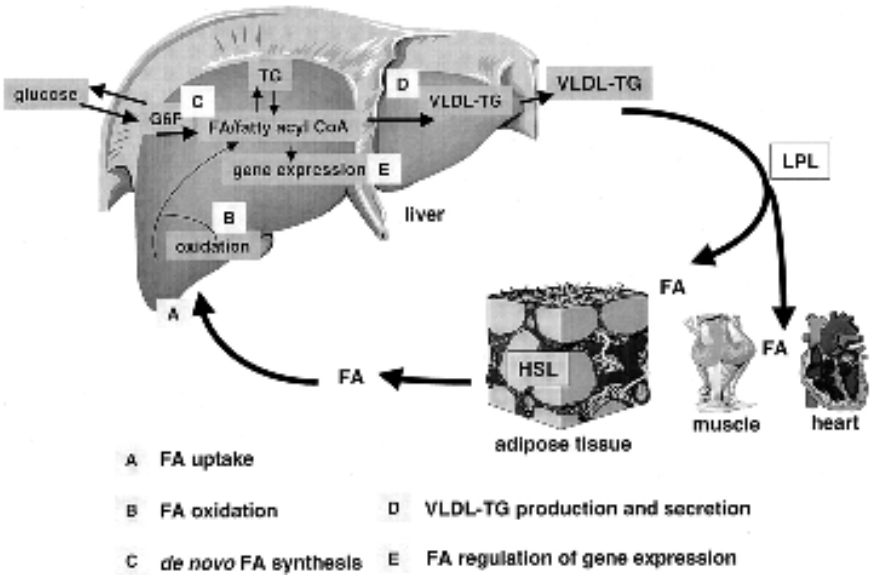

Fig. 1. Major pathways of hepatic fatty acid/triglyceride metabolism in the liver (den Boer *et al.*, 2004).

Lipids arrive at the hepatocyte surface in a number of forms, but an important source is represented by circulating free fatty acids (FFAs), deriving from lipolysis of stored TGs in adipocytes and dietary fat. FFAs are energy-rich molecules that are pivotal for a variety of cellular processes including energy storage, synthesis of cellular membranes, and generation of lipid-containing messengers in signal transduction (Reddy, 2001). Both liver and adipose tissue play a crucial role during free fatty acid metabolism and transportation. As evident from Figure 2, lipoprotein lipase (LPL) on adipocytes releases FFA from lipoprotein particles. The FFA is subsequently transported into the adipocyte and then esterified to TG for storage. Successively, stored TG undergoes lipolysis by hormone-sensitive lipase (HSL) to produce FFA for export into the plasma. At the hepatocyte, hepatic lipase (HL) produces FFA from lipoproteins which is transported into the hepatocyte along with plasma FFA. Within the liver, FFA either enter mitochondria to undergo oxidation as fuel or is esterified to TG (a storage form of three long-chain fatty acids bound to glycerol backbone by ester bonds) (Bradbury, 2006).

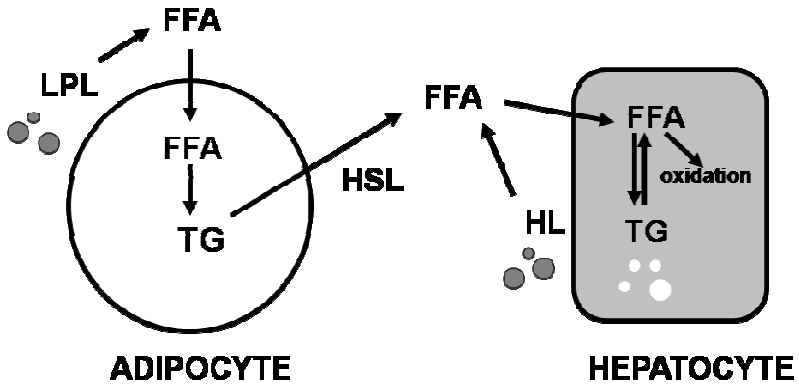

Fig. 2. Free fatty acid metabolism and transport (Bradbury, 2006).

Subsequently, depending on the availability, TGs can be stored in lipid droplets for later use or secreted into the blood in the form of VLDL-TG particles and directed toward different tissues. Plasma VLDL-TG particles consist of TGs droplets (and cholesterol esters) surrounded by phospholipids and a large glycoprotein named apolipoprotein B (apoB) (Begriche *et al.*, 2006). The assembly of apoB into VLDL is a complex process, divided into two steps. Briefly, in the first step, apoB is co-translationally lipidated in

the rough endoplasmic reticulum by microsomal triglyceride transfer protein (MTP) (Fig. 3, step 1-4). The second process includes fusion of apoB-containing precursor particles with TGs droplets to form mature VLDL-TG (Fig. 3, step 5-6). Fully lipidated apoB molecules migrate to the sinusoidal membrane of the hepatocyte and fuse with the membrane to be secreted into blood (Shelness and Sellers, 2001).

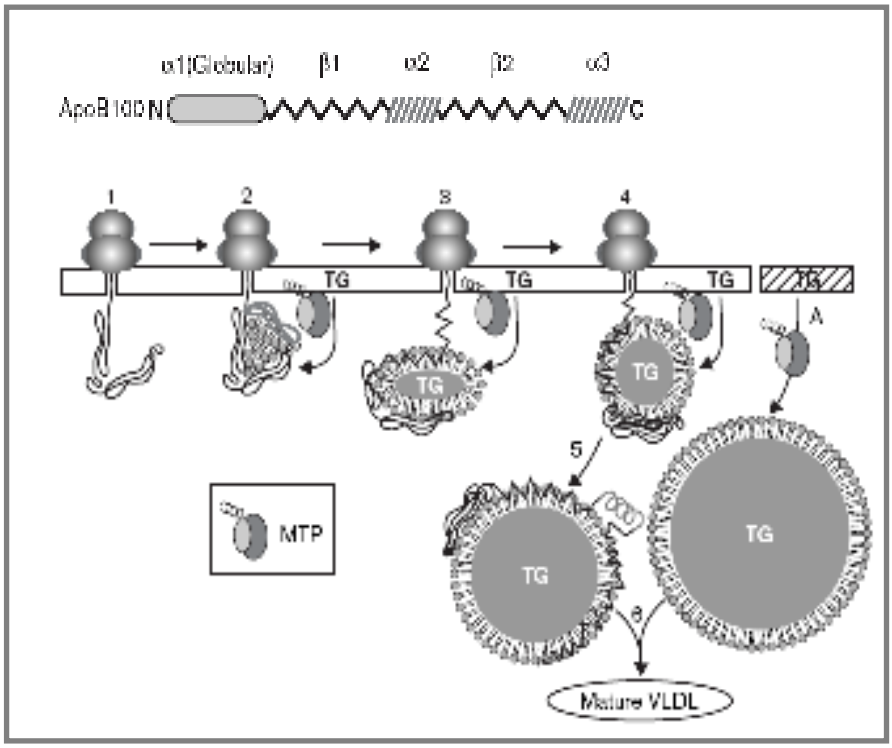

Fig. 3. Domain structure of apoB and VLDL-TG assembly (Shelness and Sellers, 2001).

Despite the complexity and a high degree of coordination of the liver lipid machinery, the overflow of any metabolite pool can lead to organ function impairment and subsequent pathologies (Nguyen *et al.*, 2008). For example, the TG content of hepatocytes is regulated by the integrated activities of cellular molecules that facilitate hepatic TG uptake, fatty acid synthesis and esterification on one hand (‘‘input’’) and hepatic fatty acid oxidation and TG export on the other (‘‘output’’). However, when ‘‘input’’ exceeds the capacity for ‘‘output’’, **hepatic steatosis** occurs. Its hallmark feature is the presence of significant amounts of TGs in hepatocytes (den Boer *et al.*, 2004). Sources of excess accumulation of triglycerides within the liver result from defects in any one of the events in the sequence from fatty acid entry to lipoprotein exit and may include:

- increased fatty acid influx into the liver from lipolysis of adipose tissue and subsequent conversion to TG;
- increased TG synthesis from elevated *de novo* synthesis of fatty acids;
- excess dietary TG associated with overeating that reach the liver as chylomicron particles from the intestine;
- reduced fatty acid oxidation;
- impaired VLDL-TG synthesis or secretion (Reddy and Rao, 2006; Anderson and Borlak, 2008).

Two major histological patterns of fat droplets accumulation in the liver parenchymal cells are defined. Macrovesicular hepatic steatosis manifests as an accumulation of large lipid vacuole filling the hepatocyte cytoplasm, resulting in peripheral displacement of the nucleus, whereas microvesicular steatosis is characterised by the presence of numerous small fat droplets without displacing the nucleus to the periphery. There are different causes which lead to these two morphological types of steatosis. Macrovesicular steatosis is related to alcoholic, obese and diabetic states as well as certain malnutrition states, such as Kwashiorkor syndrome and may manifest in *zone 3* (of the liver) or may present as panacinar with increasing severity. On the contrary, genetic or toxin-induced abnormalities in mitochondrial and peroxisomal β-oxidation of fatty acids cause microvesicular hepatic steatosis. This type tends also to be rapidly progressive and more severe (Reddy and Rao, 2006).

Non-alcoholic fatty liver disease: from steatosis to cirrhosis

Since 1845, when alcohol-induced liver steatosis was first described, the majority of cases of fatty liver disease (FLD) was attributed to the excessive use of alcohol. Throughout the recent years, research on non-alcoholic causes of FLD, diagnosed in individuals whose alcohol consumption was nil or negligible, increased exponentially and attracted considerable attention. As a consequence, FLD is now clinically categorized into two broad entities: alcoholic FLD and non-alcoholic FLD (Farrell and Larter, 2006; Reddy and Rao, 2006). The embracing term non-alcoholic fatty liver disease (NAFLD) has been adopted to cover the full spectrum of metabolic fatty

disorders, ranging from simple steatosis to steatohepatitis, advanced fibrosis and cirrhosis. The acronym NASH (**n**on-**a**lcoholic **s**teato**h**epatitis), coined by Ludwig to describe a liver disease that histologically mimics alcoholic hepatitis but occurs without abuse of alcohol, refers to a stage within the spectrum of NAFLD (Das and Kar, 2005; Ota *et al.*, 2007). In the past, histological characteristics of NASH used to be controversial and varied in the literature. As recently proposed (Neuschwander-Tetri *et al.*, 2003b), the histopathological features of non-alcoholic steatohepatitis encompass *zone 3* predominate macrovesicular steatosis in combination with hepatocyte ballooning and a mixed inflammatory infiltrate often with characteristic perisinusoidal and pericellular fibrosis. Despite the high prevalence of NAFLD and its potential for serious sequelae, the underlying etiologic factors that determine disease progression are poorly understood (Farrell and Larter, 2006). Metabolic studies in humans and animals show inextricable association with insulin resistance and features of the metabolic syndrome. Over 90% of patients with NAFLD represent at least one feature of metabolic syndrome. As lately published (Ota *et al.*, 2007), diabetes or insulin resistance may accelerate the entire pathological spectrum of NAFLD. Less commonly, NAFLD may be a result of secondary causes such as medications (e.g. corticosteroids, tamoxifen), nutritional causes (e.g. rapid weight loss) or metabolic diseases (e.g. lipodystrophy or dysbetalipoproteinaemia) (Adams and Angulo, 2005; Adams *et al.*, 2005). Remarkably, NAFLD if often diagnosed in asymptomatic persons after the detection of raised aminotransferases at a routine check-up or abnormal hepatic ultrasonography made for another purpose (e.g. suspicion of biliary disease). Even if alanine aminotransferase (ALT) and aspartate aminotransferase (AST) values are elevated in many cases, transaminases in the normal range, despite histologically significant disease, are also observed. Moreover, the presence of symptoms, usually non specific, does not appear reliably related to disease severity. Although pharmacological therapy has elicited considerable interest and different classes of drugs have been examined in human pilot studies (e.g. antioxidants, ursodeoxycholic acid, metformin, lipid lowering drugs), up till now, no accepted treatment strategy for patients suffering from NAFLD has been well established (Farrell and Larter, 2006). Taken all together, many issues remain unresolved regarding the diagnosis and treatment of NAFLD (Neuschwander-Tetri *et al.*, 2003b).

Nuclear receptors as drug targets in NAFLD

In recent years, the significance of nuclear receptors as attractive drug targets for the management of metabolic diseases has been emphasized (Tobin and Freedman, 2006; George and Liddle, 2007). Some members of the large superfamily of nuclear hormone receptors [e.g. peroxisome proliferator-activated receptors (PPARs), constitutive androstane receptor (CAR), liver X receptor (LXR), farnesoid X receptor (FXR), pregnane X receptor (PXR)] which function as ligand-activated transcription factors, are known to act as intracellular sensors for cholesterol metabolites, free fatty acids, and a range of other lipophilic molecules with critical roles in energy homeostasis, lipid metabolism and inflammation (George and Liddle, 2007). For example, involvement of PPARs in the development of hepatic steatosis and inflammation has been extensively characterized. The PPAR family of transcription factors encompasses three members: PPARα, PPARδ and PPARγ. First of all, using a nutritional model of non-alcoholic steatohepatitis in PPARα$^{-/-}$ mice demonstrated that these animals display severe hepatic steatosis, elevated serum cholesterol and TG levels, as well as reduced capacity to metabolize fatty acids (Linden *et al.*, 2001; Kashireddy and Rao, 2004a). Secondly, it has been shown that ligand-activation of PPARα, acting as a molecular sensor of endogenous fatty acids and their derivates, regulates the expression of genes encoding enzymes and transport proteins controlling lipid homeostasis, thereby stimulating β-oxidation of fatty acids and improving lipoprotein metabolism. Moreover, PPARα activation has anti-inflammatory effects via inhibition of cyclooxygenase-2 (COX-2) and interleukin-6 (IL-6) (Lefebvre *et al.*, 2006; George and Liddle, 2007). It has been also observed that ciprofibrate, a potent PPARα ligand, is able not only to prevent but also to reverse the development of the dietary-induced steatohepatitis and normalize serum aminotransferases (Rao *et al.*, 2002). In another report, a potent and selective synthetic PPARδ-agonist, GW501516, demonstrated similar protective effect improving hepatic steatosis. This receptor has been also indicated as a therapeutic target for the treatment of multiple components of the metabolic syndrome (e.g. obesity, hyperglycemia, insulin resistance, dyslipidemia). Furthermore, also PPARγ agonists seem an attractive therapeutic option as the overall effect of PPARγ activation include an increase in insulin sensitivity and glycemic control. This event is accompanied by a reduction in circulating free fatty acids (Tobin and Freedman, 2006). Additionally,

PPARγ appears to be involved in the maintenance of a quiescent phenotype of hepatic stellate cells, the characteristic relevant to the prevention of liver fibrogenesis (Marra *et al.*, 2000). To date, PPARα (clofibrate) and PPAR*γ* (thiazolidinediones: troglitazone, rosiglitazone and pioglitazone) agonists have been investigated in human pilot studies (Laurin *et al.*, 1996; Miyazaki *et al.*, 2002; Neuschwander-Tetri *et al.*, 2003a; Sanyal *et al.*, 2004; Belfort *et al.*, 2006). However, it has been revealed that these drugs have potential adverse effects. Therefore, the need for further research on larger randomized controlled trials has been underlined (George and Liddle, 2007).

Other nuclear receptors have only recently begun to be examined for their role in the pathogenesis or treatment of NAFLD. Similar effect to that of ligands of the PPARs has been observed with 1,4-bis-[2-(3,5-dichloropyridoloxy)]benzene (TCPOBOP), a ligand of constitutive androstane receptor (CAR) (a biosensor for endo- and xenobiotic compounds), another member of the nuclear receptor superfamily. It has been reported that activation of CAR by TCPOBOP reduced hepatic steatosis, serum triglyceride levels and was sufficient to attenuate inflammation in a rodent nutritional model of NASH (Baskin-Bey *et al.*, 2007).

Although 3,5,3'-triiodo-L-thyronine (T3), an agonist of another member of the steroid/thyroid hormone nuclear receptor superfamily (Germain *et al.*, 2006), resembles peroxisome proliferators (PPs), ligands of the PPARs, as well as CAR agonists, regulating serum lipid homeostasis and fat tissue metabolism (Castellan *et al.*, 1991; Hulbert, 2000), and being a potent hepatomitogen (Pibiri *et al.*, 2001; Ledda-Columbano *et al.*, 2003), its hypothetical effect on NAFLD remained largely unexplored.

Molecular basis of thyroid hormone action

The thyroid gland, whose biological importance has been recognized for centuries, produces 3,5,3',5'-tetraiodo-L-thyronine (T4) and 3,5,3'-triiodo-L-thyronine (T3) which affect numerous physiological processes (Lazar, 2003). Not only do thyroid hormones (THs) play a critical role during embryogenesis and postnatal growth (they are essential for endochondral bone formation) but also have profound influence in adult life, affecting the processes and pathways related to lipid and cholesterol handling as well as, mediating protein, carbohydrate and vitamin metabolism. Among the pleiotropic effects

exerted by THs we can also mention their influence on metamorphosis in amphibians and development of the vertebrate nervous system (Moreno *et al.*, 2008). A negative feedback system involving hypothalamus, pituitary and thyroid gland (hypothalamus/pituitary/thyroid axis) regulates exquisitely THs synthesis and secretion (Yen, 2001). T4 is the major secreted hormone but acts as a pro-hormone. The production of circulating T3, results from the activity of the iodothyronine deiodinase enzymes (selenoproteins) D1 and D2 which convert T4 to T3 by 5'monodeiodination (Oetting and Yen, 2007). On the contrary, the D3 enzyme inactivates T4 and T3 by 5'monodeiodination. Therefore, the intracellular level of T3 depends on the relative activities of these 3 deiodinases (Bassett *et al.*, 2003).

The biologically active form of thyroid hormone - triiodothyronine - acts and regulates nuclear gene expression through thyroid hormone receptors (TRs), which are members of the steroid/thyroid receptor superfamily of nuclear hormone receptors. In the mid-1980s, two research groups simultaneously published the landmark discovery, which showed that TRs were the cellular homologs (c-erbA) of v-erbA, a viral oncogene product involved in chick erythoblastosis (Sap *et al.*, 1986; Weinberger *et al.*, 1986). Acting as transcription factors, TRs bind to specific DNA sequences known as thyroid response elements (TREs), typically located in the upstream promoter regions of T3-target genes, activating or repressing transcription in response to hormone. In positively regulated target genes, TREs generally contain at least two hexameric half-sites consisting of the consensus sequence G/AGGTC/GA. In particular, TRs bind to TREs in which half-sites are arranged as direct repeats with a four nucleotide spacer (DR4), as inverted repeats with a six nucleotide spacer (IP6) or as a palindrome (PAL0) (Aranda and Pascual, 2001). Although thyroid hormone receptors are capable of binding DNA at TREs as monomers or homodimers, TRs predominantly bind as heterodimers with the retinoid X receptor (RXR), another member of the nuclear receptor superfamily. It is well established that RXR increases the DNA-binding affinity of TR (Lazar, 2003). Numerous analyses of TRs and comparison with other members of the nuclear hormone receptor superfamily have yielded thorough information on the structural features of TRs. All TRs have a similar domain organisation as that found in all nuclear hormone receptors (Fig. 4): an amino-terminal A/B domain; a central DNA-binding domain (DBD) or region C containing two zinc finger motifs intercalating with the major and minor grooves of TRE nucleotide sequences; a linker region D with a stretch of multiple

lysines necessary for nuclear translocation of the receptor; and a carboxy-terminal ligand-binding domain (LBD) (Yen, 2001).

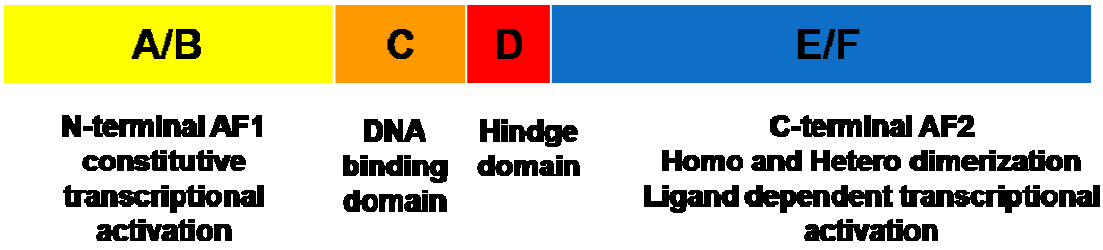

Fig. 4. A schematic representation of the functional domains of the thyroid hormone receptor (Bassett *et al.*, 2003).

More precisely, the N-terminal A/B region, highly variable both in size and sequence among various nuclear receptors, contains a transcriptional activation function, referred as activation function 1 (AF-1), that can operate autonomously. In contrast to the other activation function (AF-2) located in the LBD of liganded nuclear receptors (NRs), AF-1 can act in a ligand-independent manner when placed outside the receptor. However, in the context of its own full-length receptor, AF-1 activity is also controlled by ligand binding to the LBD (Germain *et al.*, 2006). The DBD, located in the central portion of TR, is the most conserved domain. Within the first of two zinc fingers, each composed of four cysteines coordinated with a zinc ion, there is a ‘‘P box’’. This critical region is known to be important in sequence-specific recognition of hormone response elements by different members of the nuclear hormone superfamily and contacts nucleic acids and phosphate groups within the major groove of the TRE. On the other hand, amino acids in the second zinc finger form so-called ‘‘D box’’ involved in dimerization (Aranda and Pascual, 2001). The D region, considered to serve as a hinge between the most highly conserved domains DBD and LBD, allows rotation of the DBD and permits the DBD and LBD to adopt different conformations without creating steric hindrance troubles (Oetting and Yen, 2007). Thyroid receptor activation occurs when an agonist ligand such as TH or similar compounds bind to a hydrophobic pocket in the core of its ligand-binding domain, composed of twelve conserved α-helical regions numbered from H1 to H12. Upon ligand binding the receptor undergoes a clear conformational change in the LBD, particularly in helix 12, which results in changes in TR interaction with co-activators and co-repressors (Lazar, 1993; Bleicher *et al.*, 2008).

Multiple thyroid hormone receptor isoforms and TH analogs

The human TRs are encoded by two genes, α and β, localized in human chromosomes 17 and 3, respectively. The TRα (NR1A1) and TRβ (NR1A2) genes encode mRNAs that are alternatively spliced and generate different mRNA isoforms: TRα1, α2, α3, Δα1, Δα2, β1, β2, β3, Δβ3 (Fig. 5). While it is known that TRα1, α2, β1, β2 proteins are expressed *in vivo*, the expression and physiological relevance of the other isoforms remain unclear (Ribeiro, 2008). Moreover, β3/Δβ3 locus is present only in rats, but not in other vertebrates, including humans (Williams, 2000; Harvey *et al.*, 2007).

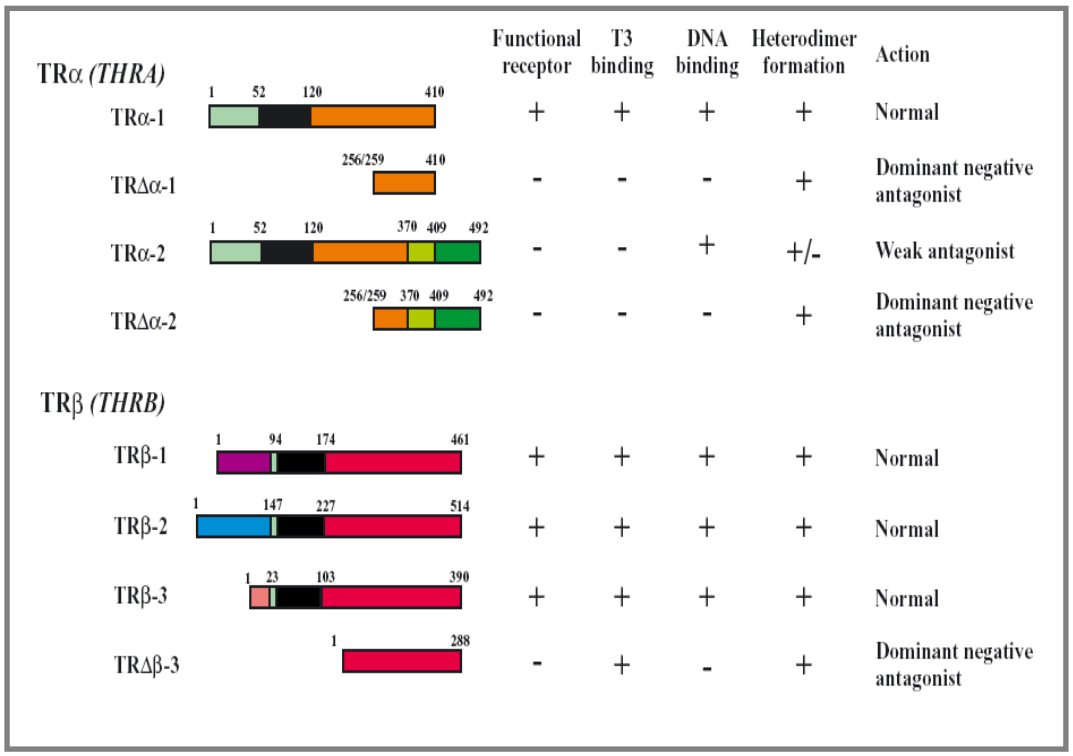

Fig. 5. Properties of major TR isoforms (Bassett *et al.*, 2003).

TR isoforms are widely distributed, although there are differences in concentrations in various tissues. For example, TRα is the dominant receptor in the brain, skeletal system and mediates most of the synergism between T3 and the sympathetic signalling pathway in the heart, whereas TRβ, abundant in liver, is supposed to be the isoform that mediates most of T3 effects on lipid metabolism and regulation of metabolic rate. Thus, it made sense to develop compounds that selectively act on one of the TRs, allowing for selective activation of different T3-mediated pathways (Ribeiro, 2008). Particular

interest has been focused on the effects of THs on lipid metabolism and the ability to lower cholesterol. However, these results occur whilst inducing a thyrotoxic state, including induction of tachycardia and arrhythmia, muscle wasting, suppression of thyroid-stimulating hormone (TSH) levels and bone mass loss; all limiting the use of THs. Since 1950s, attempts to eliminate these undesired effects were made. A promising strategy for treating lipid disorders in euthyroid individuals appeared with a new class of halogen-free high-affinity thyroid hormone agonists (Moreno *et al.*, 2008). In 1998, the synthesis of 3,5-dimethyl-4(4'-hydroxy-3'-isopropyl benzyl)-phenoxy) acetic acid, a TRβ-selective agonist was announced. This novel thyromimetic compound, named GC-1, presented some structural changes with respect to the natural hormone T3 (Fig. 6):

- the three iodine residues of T3 were replaced by methyl and isopropyl groups;
- a methylene linkage replaced the biaryl ether linkage between the two phenol groups;
- the amino acid side-chain at the 1 position changed with an oxyacetic group (Chiellini *et al.*, 1998).

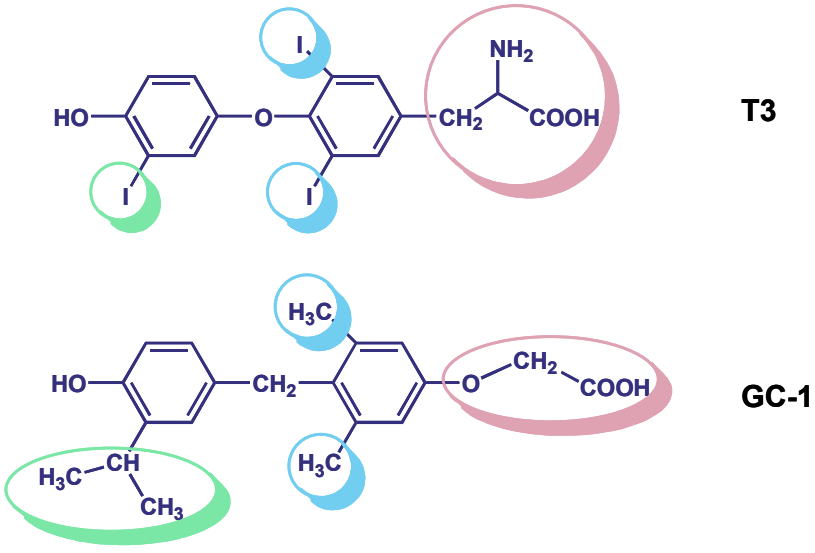

Fig. 6. Chemical structures of T3 and GC-1.

As a consequence of these modifications GC-1 binds to TRβ1 with approximately the same affinity as T3, whereas the novel thyromimetic compound binds to TRα1 with a 10-fold lower affinity. This TRβ selectivity was seen, not only in binding experiments,

but also in dose-response cellular transactivation experiments (Chiellini *et al.*, 1998). Recently, the x-ray structures of both thyroid hormone receptor isoforms as bound to natural hormone T3 and GC-1, supported by molecular dynamics simulations of the complex, permitted the proposal of a β-selectivity mechanism for GC-1. The major contributions for isoform-selective binding of GC-1 are the presence of an oxyacetic acid ester oxygen, the absence of the amino group relative to T3, the Ser/Asn active-site substitution (human (h)TRα has a Ser277 residue, which is substituted by Asn331 in hTRβ) and alternate conformations of a conserved Arg residue in the binding pocket (Arg228α/Arg282β). While in TRβ a single stable ‘‘productive’’ conformation is observed, in which GC-1 interacts effectively with Arg282, whereas this residue interacts with the carbonyl group of Asn331, in TRα, ‘‘productive’’ and ‘‘non-productive’’ conformations can be observed. The selective binding of GC-1 is related to the fact that the Ser/Asn active-site substitution increases the space available to a conserved Arg residue (Arg228) allowing it to assume multiple conformations. In the ‘‘productive’’ conformation, identical to that of TRβ, the ligand interacts strongly with the Arg228 residue and with the Ser277 by its oxyacetic oxygen. However, TRα Arg228 possesses also the ability to flip away from the ligand in ‘‘non-productive’’ conformations, which result in loss of a crucial interaction for the stabilization of the ligand (Bleicher *et al.*, 2008).

As reported in the literature, in the first studies in animal models, GC-1 showed extremely encouraging results, decreasing total serum cholesterol and triglyceride levels in hypercholesterolemic rats without any significant cardiac effects. In particular, it has been noticed that GC-1 can retain the beneficial effects of T3 at doses devoid of deleterious cardiovascular effects on heart weight, heart rate and mRNAs coding for proteins related to cardiac contraction, such as myosin heavy chain α (MHCα), MHCβ and sarcoplasmic reticulum calcium adenosine triphosphatase (Serca2) (Trost *et al.*, 2000). Additional experiments performed in cynomolgus monkeys, having a lipid metabolic profile more closely resembling that of a man, showed that the selectivity of GC-1 resulting in an improved therapeutic index for lipid lowering relative to cardiac effects is also observed in primates (Grover *et al.*, 2004). Successive studies clarified the mechanisms involved in the cholesterol-lowering effect of this selective thyromimetic compound. Experiments performed in euthyroid chow-fed mice demonstrated that GC-1 reduced serum cholesterol and triglyceride levels, increased expression of the hepatic high-density lipoprotein (HDL) receptor SR-B1, as well as

stimulated bile acid synthesis and excretion, thus regulated important steps in reverse cholesterol transport. Moreover, GC-1 at equimolar doses was even more efficient than T3 (Johansson *et al.*, 2005). In addition, it has been observed that GC-1 increases the metabolic rate, has no effect on food intake and reduces fat mass in female rats after 6 weeks of treatment, without any apparent loss of skeletal muscle mass (Villicev *et al.*, 2007).

Taking into consideration the selective hyperthyroidism of GC-1, this novel compound can be considered as a promising prototype for new drugs for the treatment of a variety of metabolic disturbances, including high lipid levels or obesity.

Animal models of hepatic steatosis and steatohepatitis

The understanding of the pathogenesis of non-alcoholic liver disease has undoubtedly improved with the help of animal models of hepatic steatosis and steatohepatitis which have provided the conceptual framework for further investigation. However, the large variety of experimental models is confusing and potentially obscures the comparison and interpretation of results (Veteläinen *et al.*, 2007). The most frequently used and particularly informative models include: genetically obese ob/ob mice, lipoatrophic mice and normal rats fed a choline-deficient, methionine-restricted (CMD) diet (Koteish and Diehl, 2002).

A naturally occurring model of non-alcoholic liver disease is represented by ob/ob mice which spontaneously develop fatty liver, due to a mutation in the ob gene, which encodes leptin, a satiety hormone secreted exclusively by adipocytes. In the absence of leptin, a sensor of fat mass, exerting anorectic and thermogenic effects through its hypothalamic receptor, ob/ob mice become obese, hyperphagic and inactive. Consequently, absence of this adipocyte-derived peptide hormone leads not only to NAFLD, but also to dyslipidemia and insulin resistance (Koteish and Diehl, 2002; Fishman *et al.*, 2007).

On the other hand, transgenic mice with differing degrees of fat loss can be used as models for lipoatrophy. An example includes mice that overexpress a truncated version, immune to down-regulation, of human sterol regulatory element binding protein-1a (SREBP-1a), a key transcriptional regulator for many genes involved in fatty acid and cholesterol biosynthesis (e.g. hydroxymethyl-glutaryl-CoA synthase and reductase, fatty

acid synthase, stearoyl-CoA desaturase, acetyl-CoA carboxylase, low density lipoprotein-receptor) (Shimano *et al.*, 1996; Shimano, 2001; Koteish and Diehl, 2002). Other strains of genetically altered mice have a generalized paucity of adipose tissue throughout life due to impaired or disordered adipocyte differentiation. This group includes:

1) A-ZIP/F-1 transgenic mice, expressing a dominant-negative protein A-ZIP/F (under the control of the adipose-specific aP2 enhancer/promoter), which inhibits the DNA binding and function of B-ZIP proteins in both the C/EBP and AP-1 families of transcription factors, critical for adipocyte growth and differentiation;
2) transgenic mice with truncated sterol regulatory element binding protein-1c (SREBP-1c) in adipose tissue (under the control of the adipocyte-specific aP2 enhancer/promoter), which is known to be implicated in adipose differentiation.

Regardless of the mechanism used to reduce the adipose tissue mass, hepatic steatosis, leptin-deficiency and severe insulin resistance are observed in all models with generalized lipoatrophy (Moitra *et al.*, 1998; Shimomura *et al.*, 1998).

Nonetheless, a particularly useful model, which emphasizes the importance of oxidative stress in the pathogenesis of hepatic steatosis and steatohepatitis, is represented by studies of animals fed the CMD diet (Lombardi *et al.*, 1968; Koteish and Diehl, 2002).

Choline homeostasis

The study of the characteristics and metabolites of choline is of meaningful importance to understand the mechanism of hepatic steatosis induced by the CMD diet. Choline, a positively charged quaternary amine (trimethyl-β-hydroxy-ethylammonium), was first isolated from ox bile (the Greek word for bile is *chole*) by Strecker in 1862. In late 1930s, Best and Huntsman discovered that choline deficiency results in fatty liver (Li and Vance, 2008). In 1998, choline was identified as an essential nutrient for humans by the National Academy of Sciences. This dietary component, required for normal function of all cells, influences stem cell proliferation and apoptosis, as well as neural tube development. Disturbed choline transport has been proposed as an important factor in neurodegenerative (e.g. Alzheimer's disease) and immunological disorders (Michel *et al.*, 2006). Utilized for the synthesis of essential lipid components of the cell

membranes - phosphatidylcholine (PC) and sphingomyelin, choline assures the structural integrity and signalling functions (Li and Vance, 2008). The Kennedy pathway (Fig. 7) for *de novo* synthesis of PC, essential for the formation of membrane phosphatidylcholine in all nucleated cells, results from the phosphorylation of the majority of cellular choline by choline kinase (CK) in the cytoplasm of the cell to phosphocholine, to which cytidine triphosphate (CTP) is added by CTP:phosphocholine cytidyltransferase (Pcyt1) to form cytidine diphosphate (CDP)-choline. The ultimate step necessary for the formation of this predominant phospholipid (>50%) in most mammalian membranes, involves the reaction of CDP-choline with diacylglycerol (DAG) in the endoplasmic reticulum, catalyzed by the membrane-bound enzyme, CDP-choline:DAG cholinephosphotransferase (CPT) (Michel *et al.*, 2006).

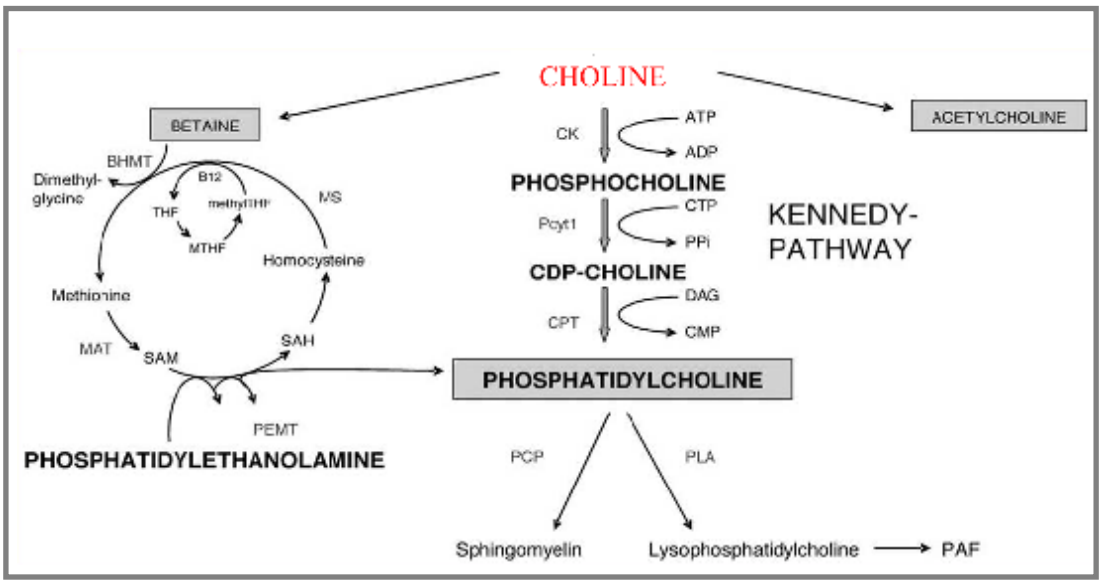

Fig. 7. Choline metabolic pathways (Michel *et al.*, 2006).

ADP, adenosine diphosphate; **ATP**, adenosine triphosphate; **BHMT**, betaine:homocysteine methyltransferase; **B12**, vitamin B12; **CDP**, cytidine diphosphate; **CK**, choline kinase; **CPT**, CDP-choline:DAG cholinephosphotransferase; **CMP**, cytidine monophosphate; **CTP**, cytidine triphosphate; **DAG**, diacylglycerol; **MAT**, methionine adenosyltransferase; **methylTHF**, 5-methyltetrahydrofolate; **MS**, methionine synthase; **MTHF**, 5,10-methylene-tetrahydrofolate; **PAF**, platelet-activating factor; **PCP**, phosphatidylcholine:ceramidecholine phosphotransferase; **Pcyt1**, CTP:phosphocholine cytidyltransferase; **PEMT**, phosphatidylethanolamine N-methyltransferase; **PLA**, phospholipase A2; **PPi**, pyrophosphate; **SAH**, S-adenosylhomocysteine; **SAM**, S-adenosylmethionine; **THF**, tetrahydrofolate.

Moreover, choline is known to be a major source of methyl groups. Betaine, one of choline's metabolites, participates in the methylation of homocysteine to form methionine, whose derivative S-adenosylmethionine (SAM) serves as an active methyl donor for many enzymatic methylations. Despite the fact that only a small fraction of dietary choline is acetylated, it plays a key role in neurons as the precursor of the neurotransmitter acetylcholine (Zeisel, 2000; Zeisel, 2006). It is important to underline that choline is not only derived from diet. During evolution, the liver has retained a backup pathway for choline moiety production from the second most abundant phospholipid membrane component, phosphatidylethanolamine (PE). PE is transformed to phosphatidylcholine in a three-step methylation by SAM, which is catalyzed by phosphatidylethanolamine N-methyltransferase (PEMT). Then, choline can be generated from PC via the action of phospholipases. It has been shown that mice that lack PEMT ($PEMT^{-/-}$), when fed the CMD diet to restrict the availability of choline, rapidly develop hepatic steatosis, severe liver damage and die from liver failure after 3 days (Li and Vance, 2008). Moreover, extensive studies on the role of the PEMT pathway in animal models support the hypothesis, that female rats are less susceptible to choline deficiency than the males. The difference is believed to be attributable to estrogen status, enhancing females' capacity to produce phosphatidylcholine via the PEMT pathway (Kirsch *et al.*, 2003; Michel *et al.*, 2006).

Mechanism of steatosis development and key molecular events while feeding the choline-deficient, methionine-restricted (CMD) diet

The functional consequence of the CMD diet is a rapid accumulation of lipids in hepatic cytosol. This phenomenon is known since the discovery of choline as a lipotrope in 1932 and triglycerides represent the main component of accumulated fatty droplets. The proposed biochemical basis of such a significant impact on liver function and lipid metabolism is attributable to impaired transport of TGs outside the hepatocytes. Reduced efficiency of VLDL-TG production occurs because choline is predominantly utilized as precursor of PC, the principal phospholipid comprising the outer coat of VLDL-TG particles (Yao and Vance, 1988; Zeisel, 1990).

Feeding the choline-deficient, methionine-restricted diet is a frequently employed nutritional model, resulting in liver injury presenting close pathological and biochemical

similarities to human NASH (Romestaing *et al.*, 2007; Veteläinen *et al.*, 2007; Rinella *et al.*, 2008). In addition to the accumulation of triglycerides occurring within 24 hours of choline restriction, numerous biochemical and molecular biology studies on the effects of the CMD diet have been performed. There is compelling evidence that one of the factors which determine how rapidly a diet deficient in choline and restricted in methionine will induce pathology is the demand for choline as methyl donor. Betaine, folate and S-adenosylmethionine concentrations are markedly diminished in livers of rats fed the choline-deficient, methionine-restricted diet (Zeisel, 1990). Concomitantly, it has been revealed that an early event in choline deficiency is the appearance of oxidized lipids, DNA and proteins, suggesting impaired oxidative balance, as well as immediate evidence of lipid peroxidation of the nuclear and mitochondrial membranes. The formation of conjugated dienes has been reported (Rushmore *et al.*, 1984) as a consequence of this free radical-mediated mechanism leading to oxidative destruction of polyunsaturated fatty acids constitutive of cellular membranes (Seki *et al.*, 2002). Oxidative damage to DNA, particularly the formation of 8-hydroxydeoxyguanosine (8-OH-dG) lesions, generally accepted as one of the most reliable markers of oxy radical-induced DNA damage (Cooke *et al.*, 2003), occurs within the time frame of lipid peroxidation (Rushmore *et al.*, 1986; Yoshiji *et al.*, 1992). Furthermore, knowing that mitochondrial β-oxidation is the dominant oxidative pathway for the removal of fatty acids under normal physiologic conditions, but also a major source of reactive oxygen species (ROS), it has been demonstrated that mitochondrial respiration, in regard to complex I-linked (NADH-dependent) respiration, is altered in association with significantly increased hydrogen peroxide (H_2O_2) leakage during choline withdrawal (Hensley *et al.*, 2000). Consequently, alterations of specific mitochondrial functions, impaired mitochondrial respiratory chain activity lead to an increased production of ROS and an impaired synthesis of ATP, critical for maintaining cellular integrity (Vendemiale *et al.*, 2001). Compared with normal liver, under fed conditions, fatty livers show also low concentration of glutathione, the main natural antioxidant essential for liver function and integrity, responsible for free radical species detoxification. This can be explained by the fact that methionine is required for the transsulfuration pathway of glutathione precursor synthesis.(Lu *et al.*, 2001; Vendemiale *et al.*, 2001). All these events are considered to have the potential to induce directly both inflammation and liver fibrosis (Browning and Horton, 2004).

Marked species-related differences in the effects of feeding the CMD have been identified. It has been demonstrated that rats display a greater propensity to develop fatty change, while inflammation and necrosis are minor features. Mice, in contrast, have less steatosis and lower hepatic triglyceride levels, but show a marked increase in inflammatory foci (Kirsch *et al.*, 2003; Kashireddy and Rao, 2004b).

Furthermore, it has been observed that choline deficiency alone is sufficient to trigger carcinogenesis, develop preneoplastic hepatocyte nodules and hepatocellular carcinoma, in the absence of any known carcinogen (Ghoshal and Farber, 1984; Ghoshal *et al.*, 1987; Chandar and Lombardi, 1988). It is noteworthy that the CMD diet-fed rats not only have a higher incidence of spontaneous hepatocarcinoma, but are also markedly sensitized to the effects of administered carcinogens (Zeisel, 1990). From the results of numerous experiments, it has been confirmed that feeding the choline-deficient, low in methionine diet strongly enhances tumour development in rats pretreated with a single initiating dose of diethylnitrosamine (DENA) (Yokoyama *et al.*, 1985; Sawada *et al.*, 1990). CMD diet effectively promotes the evolution of initiated cells to foci of altered γ-glutamyltranspeptidase (GGT)-positive hepatocytes. The expression of this enzyme, a common biochemical marker for early preneoplastic lesions, is highest in embryo livers, decreases rapidly to the lowest levels after birth and is re-expressed during the development of HCC (Shinozuka *et al.*, 1979).

AIM OF STUDY

AIM OF STUDY

Non-alcoholic fatty liver disease (NAFLD) that may develop fibrosing steatohepatitis or progress to cirrhosis, end-stage liver disease and hepatocellular carcinoma is a highly prevalent disease. Ineffectiveness of current drug therapies and an increasing need for new therapeutic tools for the treatment of NAFLD led us to investigate the effect of the thyroid hormone triiodothyronine (T3) on fatty liver and steatohepatitis. For this study, we employed a choline-deficient, methionine-restricted (CMD) dietary model in rats. In particular, we wanted to examine if:

1a. concurrent administration of the CMD diet and T3 results in the prevention of fatty liver;

1b. feeding the CMD diet followed by feeding the CMD diet containing T3 reverses CMD-induced fatty liver.

Subsequently, aware of the concomitant induction of a thyrotoxic state during T3-based therapies, we focused our attention on GC-1, an agonist of the thyroid hormone receptor β isoform, which has no significant side effects on heart rate. Strongly convinced that selective thyromimetics may offer several types of therapeutic potential and are interesting candidates for further exploration, we investigated if:

2a. co-administration of GC-1 with the CMD diet prevents CMD-induced fat accumulation;

2b. CMD dietary feeding followed by feeding the CMD diet containing GC-1 reverses fully established fatty liver.

Since the measurement and interpretation of the endogenous metabolite profile from a biological sample has been recognised as a valuable tool in life sciences, we were encouraged to:

3. extend the understanding of the mechanisms accompanying lipid accumulation and decrease in the liver during treatment with GC-1, applying a metabolomic technique. **This data was made available thanks to our collaboration with the University of Cambridge.**

MATERIALS AND METHODS

MATERIALS AND METHODS

Animals and diets

Male Fischer (F-344) rats, 6-8 weeks of age, body weight ranging from 100-125 g, purchased from Charles River (Milan, Italy) were used for the experiments. On arrival, the animals were maintained on a rodent standard diet (Standard Diet 4RF21, Mucedola, Settimo Milanese, Italy), given food and water *ad libitum* with alternating 12-hour dark/light cycles and acclimatized to laboratory conditions for a minimum of seven days before the start of the experiment. Temperature and humidity were controlled for the entire period of experimentation. All procedures were performed in accordance with the Universities Federation for Animal Welfare Handbook on the Care and Management of Laboratory Animals and the guidelines of the animal ethics committee of the University of Cagliari. After acclimatization, the rats were randomized into various experimental groups and fed as follows:

1) CMD diet (Mucedola**,** Settimo Milanese, Italy), prepared according to the original formula (Shinozuka *et al.*, 1978), containing a limited (0,2%) amount of methionine, in view of the efficient endogenous synthesis of choline from methionine;

2) CMD diet supplemented with T3 at a final concentration of 4 mg/kg of diet (Mucedola**,** Settimo Milanese, Italy);

3) CMD diet supplemented with GC-1 (synthesized as described by Chiellini *et al.* in 1998) at a final concentration of 5 mg/kg of diet (Mucedola, Settimo Milanese, Italy);

4) choline-supplemented (CS) diet (Mucedola**,** Settimo Milanese, Italy), identical to the CMD diet except that it was supplemented with choline bitartrate (1 g/kg).

For detailed components of the Standard Diet 4RF21, CS and CMD diets see **Table 1.** While eating the experimental formulas, all animals had free access to water.

	STANDARD DIET 4RF21	CS DIET	CMD DIET
Ingredients	Wheat; Maize; Soybean, dehulled extracted toasted; Corn gluten feed; Wheat straw; Fish meal; Lucerne meal; Mineral dicalcium phosphate; Calcium carbonate; Sodium chloride; Whey powder; Soybean oil; D,L-Methionine; Yeast	Sucrose; Coconut oil; Starch; Dextrine; Extracted peanut meal; Soy protein; Corn oil; Cellulose; Dicalcium phosphate; Potassium citrate; Magnesium oxide; Sodium chloride; L-Cystine	Sucrose; Coconut oil; Starch; Dextrine; Extracted peanut meal; Soy protein; Corn oil; Cellulose; Dicalcium phosphate; Potassium citrate; Magnesium oxide; Sodium chloride; L-Cystine
Vitamins	Vitamin A Vitamin D_3 Vitamin E Vitamin B_1, B_2, B_6, B_{12} Vitamin K_3 Niacin Folic acid d-Pantothenic Acid Biotin **Choline 1000 mg**	Vitamin A Vitamin D_3 Vitamin E **Choline 1000 mg**	Vitamin A Vitamin D_3 Vitamin E
Minerals	Fe (ferrous sulphate heptahydrate) Mn (manganous sulphate monohydrate) Zn (zinc sulphate monohydrate) Cu (copper sulphate pentahydrate) J (calcium iodate anhydrous) Co (basic cobaltous carbonate monohydrate)	Cu (copper sulphate pentahydrate) Se (sodium selenite)	Cu (copper sulphate pentahydrate) Se (sodium selenite)
Analysis %	Protein: 18.5 **Fat: 3.0** Fibre: 6.0 Ash: 7.0	Protein: 12.0 **Fat: 16.0** Fibre: 2.0 Ash: 3.5	Protein: 12.0 **Fat: 16.0** Fibre: 2.0 Ash: 3.5

Table 1. Components of the Standard Diet 4RF21, CS and CMD diets.

Experimental protocols

In **experimental protocol I** (Fig. 8), rats were fed the CS or the CMD diet for 1, 3, 5 and 7 days and sacrificed on the first, third, fifth and seventh day.

In **experimental protocol II** (Fig. 9), rats were fed the CS, CMD diet or the CMD diet supplemented with T3 for 1 week and sacrificed on the seventh day.

For **experimental protocol III** (Fig. 10), rats were fed the CMD diet for 10 weeks and then divided into two groups. The first group was maintained on the CMD diet for an extra week, while the second group was fed the CMD+T3 diet. Rats on the choline-supplemented (CS) diet for 11 weeks were used as the control group. Animals were sacrificed at the end of the eleventh week.

In **experimental protocol IV** (Fig. 11), rats were fed the CS, CMD diet or the CMD diet supplemented with GC-1 for 2 weeks and sacrificed on the fourteenth day.

For **experimental protocol V** (Fig. 12), rats were fed the CMD diet for 10 weeks and then divided into two groups. The first group was maintained on the CMD diet for another two weeks, while the second group was fed the CMD+GC-1 diet. Rats on the choline-supplemented (CS) diet for 12 weeks were used as the control group. Animals were sacrificed at the end of the twelfth week.

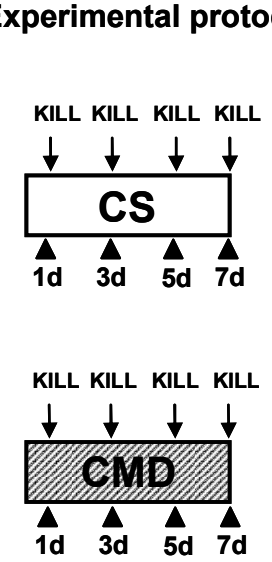

Fig. 8. Schematic representation of the design of the experimental protocol I. 5 to 6 male Fischer rats (F-344) per group were used.

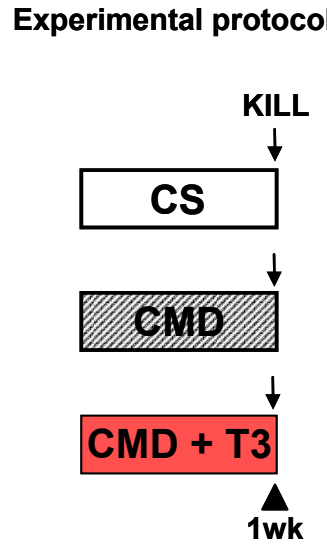

Fig. 9. Schematic representation of the design of the experimental protocol II. 5 to 6 male Fischer rats (F-344) per group were used.

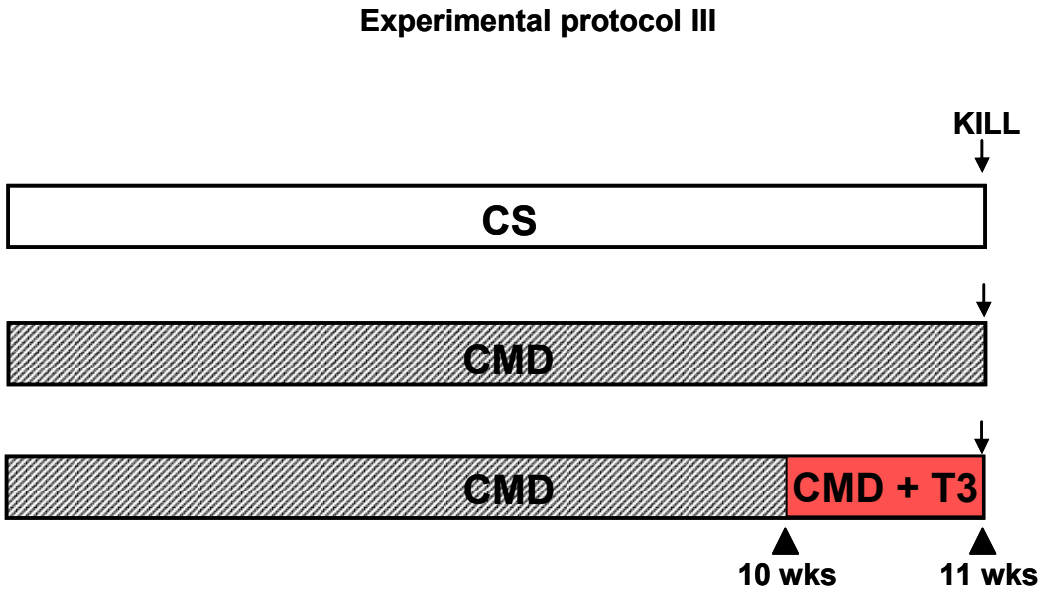

Fig. 10. Schematic representation of the design of the experimental protocol III. 5 to 6 male Fischer rats (F-344) per group were used.

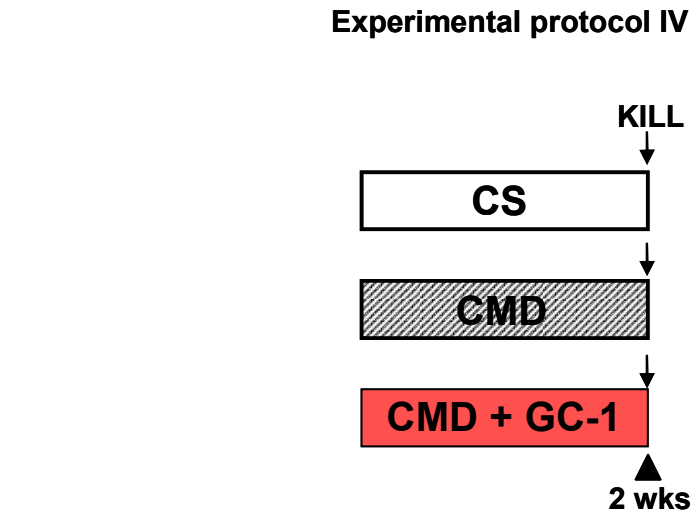

Fig. 11. Schematic representation of the design of the experimental protocol IV. 5 to 6 male Fischer rats (F-344) per group were used.

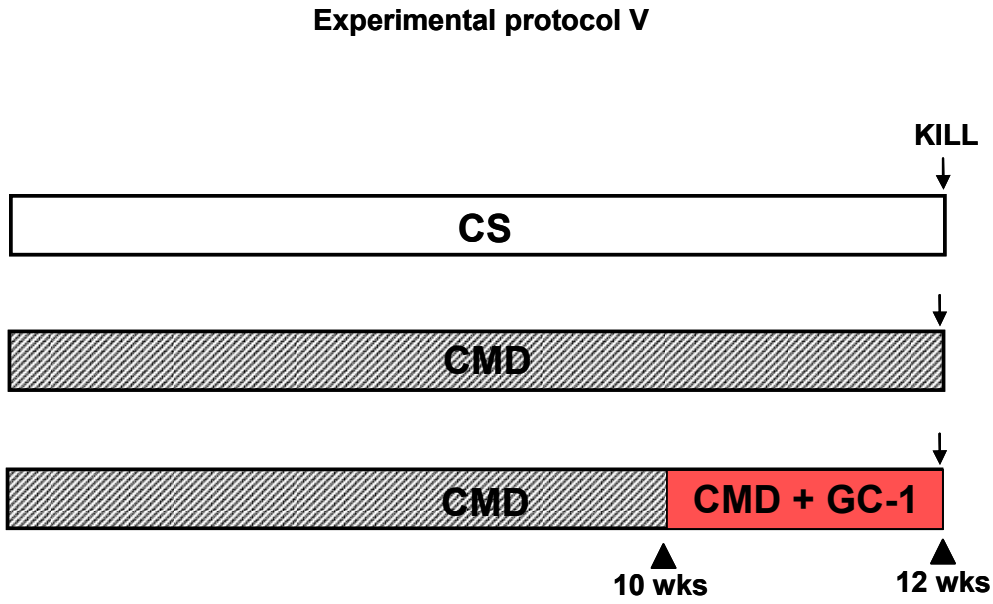

Fig. 12. Schematic representation of the design of the experimental protocol V. 5 to 6 male Fischer rats (F-344) per group were used.

Histology

Immediately after the animals were killed, sections of the liver were fixed in 10% buffered formalin and paraffin-embedded for staining with hematoxylin-eosin for routine morphology and the evaluation of hepatic steatosis. The remaining liver was snap-frozen in liquid nitrogen and kept at -80 °C until use.

Lipid peroxidation assay (LPO assay)

Approximately 100 mg of liver tissue was homogenized with an Ultra Turrax T8 stirrer (IKA Labortechnik, Staufen, Germany) in ice-cold 20 mM Tris-HCl buffer (pH 7.4) to produce a 1/10 homogenate. The crude homogenate was centrifuged at 7000 rpm for 15 minutes at 4°C. Aliquots of the supernatant were used either for protein determination or to calculate lipid peroxidation.

Lipid peroxidation was assessed by measuring the concentration of malondialdehyde (MDA) and 4-hydroxyalkenals (4-HDA) using the Bioxytech® LPO-586 kit^{TM} (Oxis International, Portland, OR, USA). This kit takes advantage of a chromogenic reagent (N-methyl-2-phenylindole, R1) which reacts with MDA and 4-HDA at 45°C yielding a stable chromophore with maximal absorption at a wavelength of 586 nm. The assay was conducted according to the manufacturer's instructions to minimise undesirable artifacts.

Determination of hepatic TGs

Lipid extraction and measurement of TGs was performed according to Schroeder-Gloeckler *et al.* (2007). Liver samples were homogenized in 0.5M NaCl, and a 200 µl aliquot of the homogenate was mixed with 500 µl of methanol and 250 µl of chloroform. Following centrifugation, the lower, organic phase was collected. Complete extraction of any residual lipids was achieved by re-extracting with 250 µl chloroform:methanol (9:1). The organic phase was separated by centrifugation and combined with the first extraction. Samples were dried under flowing nitrogen. The

lipids were dissolved in a solution of 90% isopropanol:10% Triton X-100 (2%) to disperse the TGs for assay.

Taking into consideration that triglycerides, esters of fatty acids and glycerol, do not circulate freely in plasma, the most common methods for triglycerides determination involve their enzymatic or alkaline hydrolysis to glycerol and free fatty acids, followed by either colorimetric or fluorometric measurement of the glycerol released. In our study, TGs were measured colorimetrically using a commercially available kit from Sigma-Aldrich (Serum Triglyceride Determination Kit-TR0100, Sigma-Aldrich, Milan, Italy). We followed the procedure of enzymatic hydrolysis by lipase.

Triglyceride Assay Enzymatic Reactions:

$$\text{triglycerides} \xrightarrow{\text{lipoprotein lipase}} \text{glycerol + fatty acids}$$

$$\text{glycerol + ATP} \xrightarrow{\text{glycerol kinase}} \text{glycerol-1-phosphate + ADP}$$

$$\text{glycerol-1-phosphate + } O_2 \xrightarrow[\text{oxidase}]{\text{glycerol phosphate}} \text{dihydroxyacetone phosphate + } H_2O_2$$

$$H_2O_2 + \text{4-aminoantipyrine + ESPA} \xrightarrow{\text{peroxidase}} \text{quinoneimine dye + } H_2O$$

ESPA: sodium N-ethyl-N-(3-sulfopropyl)m-anisidine

A quinoneimine dye shows an absorbance maximum at 540 nm.

Biochemical analysis: serum TGs, alanine aminotransferases (ALTs) and aspartate aminotransferases (ASTs)

Immediately after sacrifice, blood samples were collected from the inferior vena cava, centrifuged at 1500 rpm for 20 minutes and serum was analyzed for TGs, ASTs, and ALTs, using a commercially available kit from Sigma Diagnostics (Sigma-Aldrich).

Northern blot analysis

Total RNA was extracted from rat liver by homogenization with TRIzol isolation reagent (Invitrogen, San Giuliano, Milan, Italy). 30 μg of total RNA was loaded on a 1% formaldehyde/agarose gel containing ethidium bromide for RNA detection at a UV lamp and blotted on Hybond-XL membrane (Amersham Biosciences, Little Chalfont, Buckinghamshire, UK). RNA concentration was determined spectrophotometrically at 260 nm. Probe for 18S was prepared from total RNA using SuperScript TM III One-Step RT-PCR System with Platinum TaqDNA Polymerase (Invitrogen). Polymerase chain reaction (PCR) primers for 18S were as follows: forward, CATTCGAACGTCTGCCCTAT; reverse, CCCTCTTAATCATGGCCTCA. Probes for peroxisomal acyl-CoA oxidase (ACO), mitochondrial carnitine-palmitoyltransferase1A (CPT1A), mitochondrial trifunctional enzyme-alpha subunit (MTPα), and mitochondrial trifunctional enzyme-beta subunit (MTPβ) were prepared from total RNA, reverse-transcribed with Thermo-Script RTPCR System (Invitrogen Carlsbad, CA, USA) and PCR amplified with Platinum *Taq*DNA Polymerase (Invitrogen) using primers detailed in **Table 2.** DNA probes were labeled with [α-^{32}P]dCTP by random priming (Ready to go DNA labeling beads; Amersham Biosciences). Unincorporated nucleotides were removed with Microspin G50 columns (GE Healthcare, Slough, Berkshire, UK). Membranes were exposed to autoradiographic film (Eastman Kodak, Rochester, NY, USA; Sigma Chemical, St. Louis, MO, USA).

PRIMER SEQUENCES	
ACO peroxisomal acyl-CoA oxidase	**FORWARD** TTGGGATCCCACTGCTGTGAGAATA **REVERSE** AACTATATTTGGCCAATTTTGTGGAACC
CPT1A mitochondrial carnitine-palmitoyltransferase1A	**FORWARD** CAAGGACATGGGCAAGTTTT **REVERSE** GGCACTGTTCTCAGCATTGA
MTP-α mitochondrial trifunctional enzyme-alpha subunit	**FORWARD** TGACGCTGTGAAGACTGGAC **REVERSE** TGTTGCTGGCGAAGATACAG
MTP-β mitochondrial trifunctional enzyme-beta subunit	**FORWARD** CAGCTGTCCAGACCAAGTCA **REVERSE** TCCTTCATCCTGTGCCTTCT
18S	**FORWARD** CATTCGAACGTCTGCCCTAT **REVERSE** CCCTCTTAATCATGGCCTCA

Table 2. Primer sequences.

Western blot analysis

Total cell extracts were prepared from frozen livers powdered in liquid nitrogen cold mortar. Equal amounts of powder (~50 mg) from three different animals were pooled per each sample point and re-suspended in 1 ml Triton lysis buffer (1% Triton X-100, 50 mM Tris-HCl pH 7.4, 140 mM NaCl, 1 mM EDTA, 1 mM EGTA, 1 mM DTT, 1 mM PMSF, 5 mM iodoacetic acid, 10 mg/ml each of aprotinin, pepstatin, leupeptin). Several protease inhibitors were added to the isolation buffer to minimize protein degradation during the isolation protocol. After vortexing, extracts were incubated 30 minutes on ice, centrifuged at 12000 rpm at 4°C, and the supernatants were recovered. All inhibitors used were purchased from Boehringer Mannheim (Mannheim, Germany) with the following exception: PMSF, NaF, and DTT, which were purchased from Sigma Chemical (St. Louis, MO, USA), and iodoacetic acid, which was from ICN Biomedicals (Irvine, CA, USA). The protein concentration of the resulting total extracts was determined according to the method of Bradford (1976) using bovine serum albumin as standard (DC Protein Assay, Bio-Rad Laboratories, Hercules, CA, USA).

For immunoblot analysis, equal amounts (from 100 to 150 µg/lane) of proteins were electrophoresed on SDS 12% or 8% polyacrylamide gels (Sigma Chemical, St. Louis, MO, USA). Acrylamide and bis-acrylamide were purchased from ICN Biomedicals (Irvine, CA, USA). After gel electrotransfer onto nitrocellulose membranes (Osmonics, Westborough, MA, USA) to ensure equivalent protein loading and transfer in all lanes, the membranes and the gels were stained with 0.5% (w/v) Ponceau S red (ICN Biomedicals, Irvine, CA, USA) in 1% acetic acid and with Coomassie blue (ICN Biomedicals, Irvine, CA, USA) in 10% acetic acid, respectively. After blocking with 5% non-fat dry milk or 5% BSA in Tris-buffered saline/Tween 20 (Sigma Chemical, St. Louis, MO, USA) at room temperature for 1 hour or overnight at 4°C, membranes were washed in TBS-T and then incubated with the appropriate primary antibodies diluted in blocking buffer. Whenever possible the same membrane was used for detection of the expression of different proteins. Depending on the origin of primary antibody, filters were incubated with anti-mouse, anti-rabbit or anti-goat horseradish peroxidise-conjugated immunoglobulin G (IgG; Santa Cruz Biotechnology, Santa Cruz, CA, USA). Immunoreactive bands were identified with a chemiluminescence detection system, as described by the manufacturer (Supersignal Substrate; Pierce, Rockford, IL, USA).

The intensity of the bands was quantified using Scion Image (NIH, Scion Corporation, Bethesda, USA)

Antibodies

Following primary antibodies were used:

- mouse monoclonal antibodies against actin (clone AC40; Sigma Chemical);
- rabbit polyclonal antibodies against L-FABP (Abcam, Cambridge, UK), signal transducer activator of transcription 3 (STAT 3), phospho-STAT 3 (Tyr705), stress-activated protein kinase (SAPK)/Jun N-terminal kinase (JNK), phospho-SAPK/JNK (Cell Signaling Technology, Beverly, MA, USA);
- goat polyclonal antibodies directed against cyclooxygenase-2 (COX)-2 (M-19) (Santa Cruz Biotechnology).

Statistical analysis

Instant software (Instat; GraphPad, San Diego, CA, USA) was used to analyze the data. One-way analysis of variance (ANOVA) with *post hoc* analysis using Tukey's multiple comparison test was used for parametric data. The results of multiple observations are presented as the means ± SE of at least 2 separate experiments. A value of $P<0.05$ was regarded as a significant difference between groups.

Ultra-performance liquid chromatography-quadrupole time-of-flight-mass spectrometry (UPLC-QTOF-MS)

Sample Preparation

Liver tissue was harvested from male Fischer (F-344) rats on CMD, CMD+GC-1, CS, and rodent standard (Standard Diet 4RF21) diets. Tissue was examined for the CMD, CMD+GC-1 groups after 3, 7, 14 days (n=5 for each) and for the CS (n=3 for each) and standard diet groups (n=5 for each). In order to separate lipids from water soluble metabolites, frozen liver (100 mg wet weight) was ground in liquid nitrogen and tissue samples were subjected to methanol and chloroform extraction in a 2:1 ratio. Then, lipid samples were re-dissolved in a 1:1 water:choloroform mixture for mass spectral analysis.

UPLC-QTOF-MS

The total lipid extracts were analyzed on a Waters (Milford, MA, USA) Q-TOF Ultima mass spectrometer coupled to an Acquity UPLC system. Samples were maintained in the autosampler prior to injection. A Bridged Ethylene Hybrid (BEH) C8 2.1 x 100 mm column (Waters; Milford, MA, USA) with 1.7 μm particle size was used at 65 ºC. Solvent A (water, 10 mM NH_4Ac, 0.01% HCOOH) and solvent B (LC/MS grade acetonitrile/isopropanol 5:2, 10 mM NH_4Ac, 0.01% HCOOH) were run from 60% B to 100% B in 8 minutes and held at 100% for 2 minutes before re-equilibrating the column at the starting conditions. The flow rate was 600 μl/min and the eluent was split two ways with one part going to waste and the other to the mass spectrometer. The resulting injection time was 12.5 minutes. The Ultima mass spectrometer (Waters; Milford, MA, USA) was operated in positive electrospray ionisation (ESI) mode. Data was collected between 80 and 1500 Da, with a scan time of 0.5 seconds. The source temperature was set at 100ºC and nitrogen was used as desolvation gas (~800L/h) at 300ºC. The voltages of the sampling cone and capillary were 35V and 3.2kV, respectively. Samples were analyzed in a randomized order with injection volumes of 2, 4, 6 and 8 μL. A blank followed by a pooled quality control sample was run between every 10 analyses to ensure instrumental stability was maintained through the course of data acquisition.

Statistical analysis

Data from UPLC-QTOF-MS analysis were pre-processed and aligned by using XCMS (various forms (X) of chromatography mass spectrometry) according to the literature (Smith *et al.*, 2006). Retention corrected peak groups were then used as input into SIMCA-P version 11.5 (Umetrics, Umea, Sweden). Principal component analysis (PCA) models were initially built to look for outliers, and subsequently supervised partial least squares-discriminant analysis (PLS-DA) modelling was performed.

RESULTS AND DISCUSSION

RESULTS AND DISCUSSION

AIM 1a

Effect of T3 on the prevention of CMD-induced fatty liver

The starting point for examining the potential effect of T3 on the prevention of fatty liver was the establishment of the dynamics of fat accumulation in rats fed the CMD diet. For this purpose, we designed and followed **the experimental protocol I**. The macroscopic appearance of the livers from the animals fed the CMD diet for 3, 5 and 7 days resulted enlarged, pale or yellow blotchy on the surface, suggesting deposits of hepatic fat compared to the livers of the animals fed the CS for the same time period. These characteristics were not evident after 1-day-feeding with the CMD or CS diet. After calculating the liver-to-body weight ratio in animals fed the CMD or CS diet for 1, 3, 5 or 7 days, we observed that after only 3 days this parameter was significantly higher in the CMD diet-fed rats when compared to the CS diet-fed animals ($P<0.005$) (Fig. 13). This difference was further increased after 5 and 7 days of feeding the CMD or CS diet ($P<0.001$) (Fig. 13). Successively, hematoxylin-eosin stained liver sections were used to confirm gradual fat accumulation and evaluation on a semi-quantitative basis was performed. The system devised for this study scored steatosis according to the percentage of hepatocytes showing lipid accumulation as follows: 0: 0%; 1: 0% to 33%; 2: 33% to 66%; 3: 66% to 100% (a grading system proposed by Brunt *et al.*, 1999). We remarked that after 7 days of the CMD diet feeding, the highest level of the severity of hepatic steatosis (grade 3) was reached (Fig. 14). Interestingly, we also noted a difference in the distribution of fat accumulation. Hepatic steatosis resulted more severe in the left lateral lobe than in the middle lobe (terminology of liver anatomy according to Higgins and Anderson, 1931).

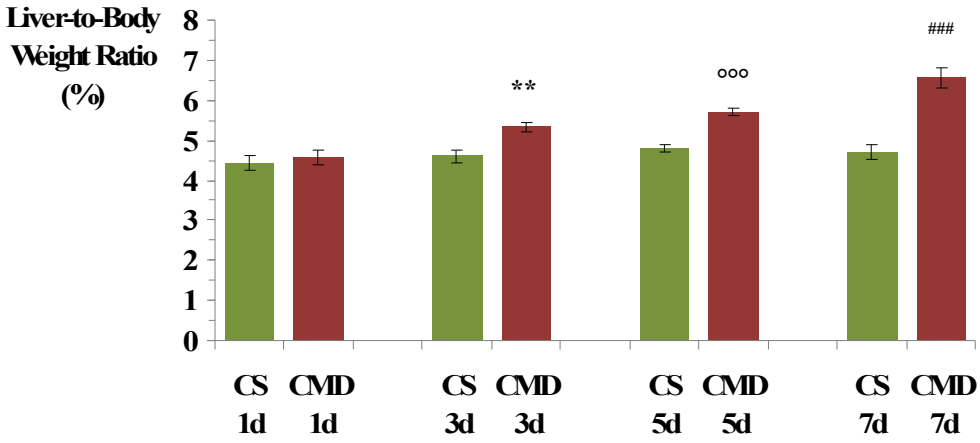

Fig. 13. Liver-to-body weight ratio of rats fed the CS or CMD diet for 1, 3, 5 and 7 days. Data is presented as mean ± SE; 5 rats per group. $^{**}P<0.005$ *vs.* CS 3d, $^{°°°}P<0.001$ *vs.* CS 5d, $^{###}P<0.001$ *vs.* CS 7d.

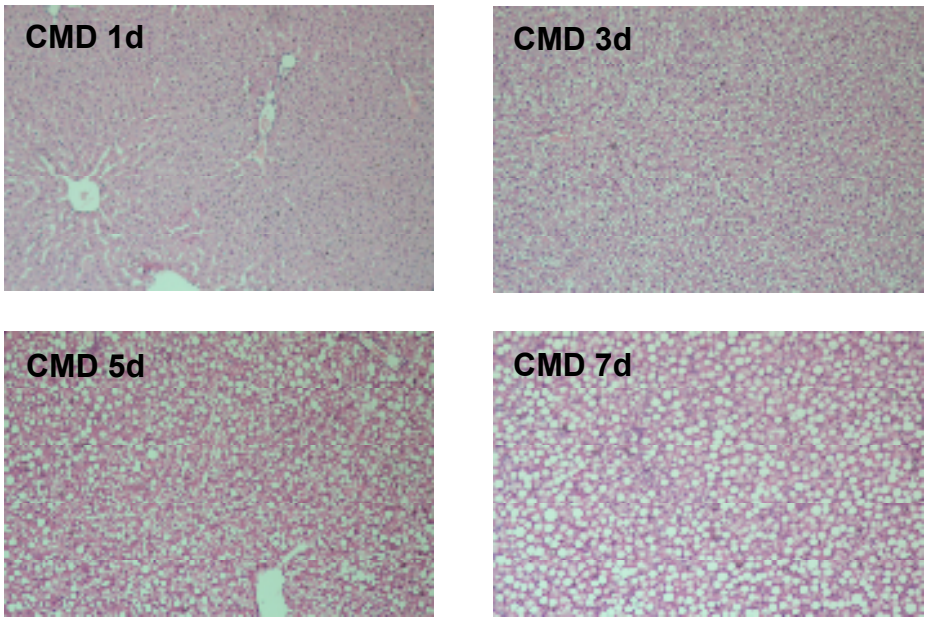

Fig. 14. Histological pattern (hematoxylin-eosin stained) of liver sections from rats fed the CMD diet for 1, 3, 5, 7 days (original magnification x10).

In order to examine the therapeutic potential of T3 in the treatment of CMD-induced steatosis, we studied the effect of concurrent administration of the CMD diet and T3 on the prevention of fatty liver. To test this hypothesis we used the **experimental protocol II**. We observed that in all experimental groups, physical activity and behaviour were similar. Appearance of animals remained healthy. No significant change in body weight occurred in rats fed the CMD diet for 1 week when compared to the CS diet-fed animals (Table 3). However, depriving rats of choline and methionine for seven days caused an ~25% increase of liver weight. The liver-to-body weight ratio was higher in the CMD diet-fed rats compared to the CS diet-fed and CMD+T3 diet-fed animals ($P<0.001$) (Table 3). While the CMD+T3 diet-fed rats had a serum triglyceride level similar to that of CMD-diet rats (Table 4), the mean body weight, liver weight and liver-to-body weight ratio were significantly less than that of the CMD diet-fed rats (Table 3).

It is well known that serum biochemical parameters provide helpful information in assessing liver damage. Alterations of the hepatocellular membrane integrity due to hepatocyte injury or metabolic disturbances (hepatic glycogen and lipid accumulation) result in a release of soluble cytosolic enzymes (out of the cytoplasm) into peripheral blood causing their increase when measured. Currently, alanine aminotransferase (ALT, formerly SGPT; found in the cytosol) and aspartate aminotransferase (AST, formerly SGOT; found in both the cytosol and mitochondria) are widely employed examples of such hepatic “leakage” enzymes. Moderate to marked increase in serum ALT and AST is observed during hepatocellular injury. However, having both cytosolic and mitochondrial isoforms, AST requires relatively severe forms of liver necrosis for its increase to occur compared to ALT. Nonetheless, ALT is recognised as more specific for the hepatocytes because of its high activity in the hepatocellular cytoplasm (Ramaiah, 2007).

As far as biochemical parameters are concerned, serum ALT and AST were increased in the CMD diet-fed animals compared to the CS diet-fed rats, whereas feeding the CMD+T3 diet caused a decrease in the levels of serum ALT and AST compared to the CMD diet-fed rats (Table 4).

Treatment	Body Weight (g)	Liver Weight (g)	Liver-to-Body Weight Ratio (%)
CS	144.2 ± 2.0	6.42 ± 0.19	4.51 ± 0.03
CMD	147 ± 2.5	8.09 ± 0.15 ***	5.53 ± 0.06 ***
CMD+T3	115.0 ± 2.4 ###	5.81 ± 0.35 ###	4.72 ± 0.14 ###

*P<0.05, **P<0.005, ***P<0.001 *vs.* CS

#P<0.05, ##P<0.005, ###P<0.001 *vs.* CMD

Table 3. Effect of T3 on body weight, liver weight, liver-to-body weight ratio in rats fed the CMD diet for 1 week. Values are expressed as means ± standard error (SE) of 5 to 6 animals per group.

Treatment	TG (mg/dl)	AST (U/L)	ALT (U/L)
CS	186.8 ± 11.9	124.5 ± 5.1	32 ± 1.9
CMD	136.4 ± 18.2 *	149 ± 2.1 **	57 ± 4.6 **
CMD+T3	122.2 ± 15.8 *	125.2 ± 7.2 #	42 ± 2.8 #

*P<0.05, **P<0.005, ***P<0.001 *vs.* CS

#P<0.05, ##P<0.005, ###P<0.001 *vs.* CMD

Table 4. Effect of T3 on serum levels of TGs, ALTs, and ASTs in rats fed the CMD diet for 1 week. Values are expressed as means ± standard error (SE) of 5 to 6 animals per group.

Histological examination was the successive step. As evident from Figure 15, livers of the CMD diet-fed rats showed severe macrovesicular steatosis with the presence of abundant fat droplets involving all hepatic lobules, whereas no pathological changes were seen in the CS diet-fed animals. The rapid accumulation of hepatic TGs confirmed by biochemical determination, is recapitulated in Figure 16. Histological examination (Fig. 15) and biochemical determination of hepatic TG content (Fig. 16) showed an almost complete absence of lipid accumulation in the CMD+T3 diet-fed rats. It demonstrates that T3 completely prevents the induction of hepatic steatosis by the CMD diet. Moreover, as previously mentioned, prevention of steatosis by T3 is accompanied by a decrease in the levels of serum ALT and AST compared to the CMD diet-fed rats (Table 4).

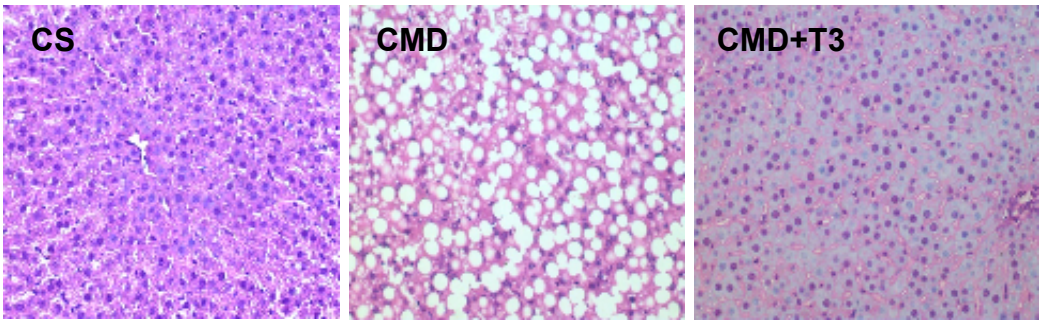

Fig. 15. Representative histology of liver tissue. Hematoxylin-eosin stained liver sections from rats fed the CS, CMD and CMD+T3 diet for 1 week (original magnification x20).

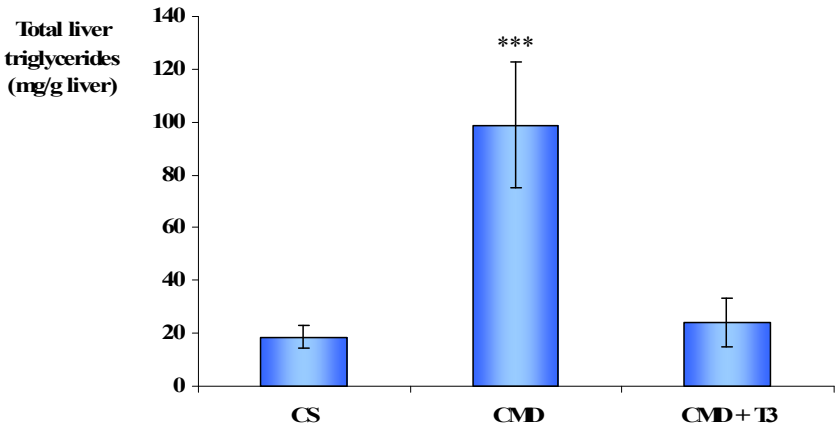

Fig. 16. Hepatic triglyceride content. Values are expressed as means ± SE; 5 rats per group. $^{***}P<0.001$ *vs.* CMD+T3 and CS. Difference between CS and CMD+T3 is not significant.

Successively, we sought an explanation for the serum and hepatic triglyceride-lowering effects of T3 by assessing the hepatic expression of genes involved in fatty acid turnover. We investigated if the prevention of hepatic steatosis by T3 depends on the ability of the liver to enhance fatty acid oxidation to get rid of the excess fatty acids. Although fatty acids can undergo oxidation via different mechanisms, most of them are degraded by means of β-oxidation, which occurs in both mitochondria and peroxisomes (Fig. 17).

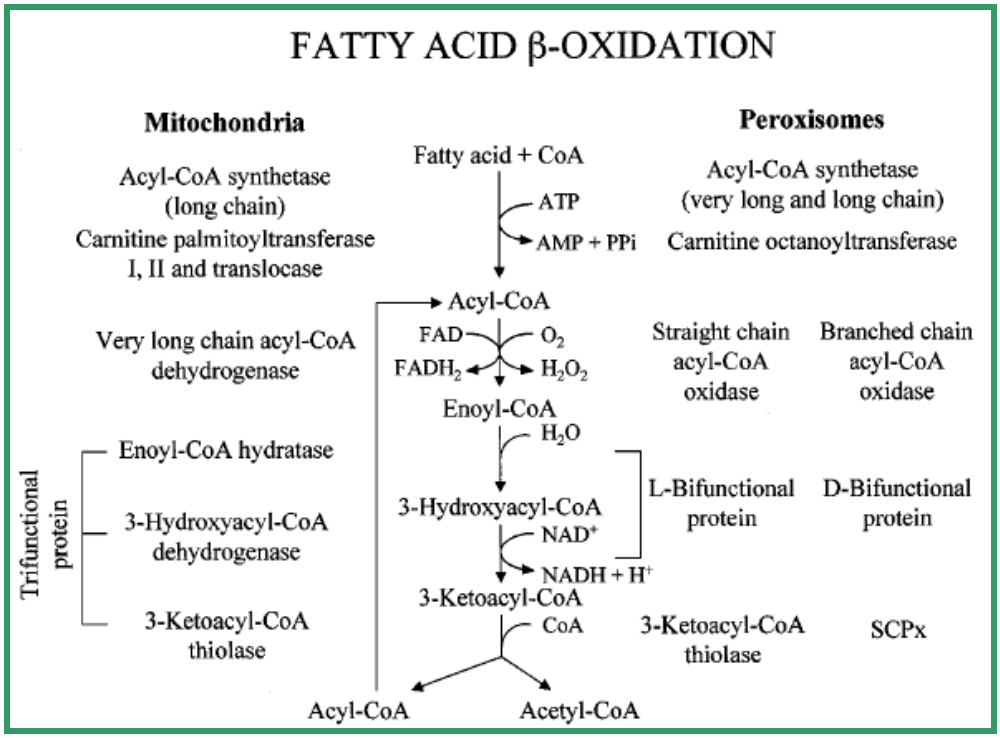

Fig. 17. Mitochondrial and peroxisomal β-oxidation systems (SCPx, sterol carrier protein x) (Reddy and Hashimoto, 2001).

Mitochondrial β-oxidation, which results in shortening of fatty acids progressively into acetyl-CoA subunits, is primarily involved in the oxidation of the bulk of short-chain ($<C_8$), medium-chain (C_8-C_{12}) and long-chain (C_{12}-C_{20}) fatty acids. Then, acetyl-CoA subunits either enter the tricarboxylic acid cycle (Krebs cycle) for further oxidation to water and carbon dioxide or condense to ketone bodies (acetoacetate, acetone, β-hydroxybutyrate) in liver that serve as oxidizable energy substrates for extrahepatic tissues, especially during starvation (Reddy and Hashimoto, 2001). Mitochondrial β-oxidation requires two steps: the first one is the transference of the acyl group from the

long chain fatty acid to carnitine and then the transport into the matrix; the second one is the intramitochondrial chain shortening consisting of a repeating circuit of four sequential reactions: 1) dehydrogenation; 2) hydration; 3) second dehydrogenation; 4) thiolytic cleavage (Serviddio *et al.*, 2007).

One of the major pathways leading to increased mitochondrial fatty acid oxidation involves activation of the rate-limiting enzyme, carnitine-palmitoyltransferase1A (CPT1A). CPT1A, the outer enzyme of the CPT system, converts long-chain fatty acyl-CoAs to acylcarnitines for translocation across the mitochondrial membrane (Reddy and Rao, 2006). Therefore, being the mitochondrial gateway for fatty acids, CPT1A is the main controller of the hepatic β-oxidation flux (Serviddio *et al.*, 2007). Jansen *et al.* (2000) have already shown that the thyroid hormone (T3) stimulates CPT1A transcription much more in the liver than in non-hepatic tissues.

Mitochondrial β-oxidation is also rate-regulated by the mitochondrial trifunctional protein (MTP) complex which carries out the second, third and fourth β-oxidation steps (Fig. 17). MTP is a hetero-octomer made up of four α-subunits with long-chain enoyl-CoA hydratase and 3-hydroxyacyl-CoA dehydrogenase activities (MTP-α), and four β-subunits with long-chain 3-oxo-/or keto-thiolase activity (MTP-β) (Reddy and Hashimoto, 2001). Analysis of the histopathological changes in the homozygous null mice for the α-subunit of MTP revealed that MTP-$\alpha^{-/-}$ mice develop hepatic steatosis immediately after birth and die suddenly 6-36 hours after birth (Ibdah *et al.*, 2001).

Partial oxidation, streamlined exclusively toward the metabolism of less abundant and relatively more toxic and biologically active very-long-chain fatty acids (containing 20 or more carbon atoms, $>C_{20}$), 2-methyl-branched fatty acids, dicarboxylic acids, prostanoids and C_{27} bile acid intermediates, occurs in peroxisomes. The presence of a fatty acid β-oxidation system in these cell organelles was described for the first time in glyoxysomes of germinating castor bean seedlings. Seven years later, a similar system, outside the mitochondrial compartment, was found in rat liver peroxisomes. Since then, it became evident that both mitochondrial and peroxisomal β-oxidation exist in the same cell. Despite being catalyzed by different enzymes encoded by different genes and having different roles, both pathways are functionally correlated (Reddy and Hashimoto, 2001). In fact, peroxisomal β-oxidation is preferentially involved in the chain shortening of very-long-chain fatty acids, and thus generating substrates for further completion of oxidation in mitochondria (Wanders, 2004). Distinctive differences between peroxisomal and mitochondrial oxidation pathways reflect the fact

that the first dehydrogenation of mitochondrial β-oxidation is replaced with an oxidation catalyzed by acyl-CoA oxidase (ACO), the rate-limiting enzyme of peroxisomal β-oxidation, converting very-long-chain fatty acyl-CoAs to their corresponding *trans*-2-enoyl-CoAs. This reaction results in the formation of H_2O_2 rather than NAD^+ (Fig. 17) (Nguyen *et al.*, 2008). It is of relevant importance to mention that mice with a disrupted ACO gene exhibit severe steatohepatitis (Fan *et al.*, 1998).

Therefore, the effect of T3 on the expression of genes involved in peroxisomal and mitochondrial fatty acid oxidation was evaluated. As far as peroxisomal β-oxidation is concerned, we observed that ACO mRNA expression levels in the liver were slightly lower in CMD rats compared to the CS diet-fed animals, whereas in the CMD+T3 diet-fed rats ACO mRNA expression levels resulted strongly induced (Fig. 18). On the other hand, the mRNA levels of the key genes involved in mitochondrial β-oxidation: CPT1A, MTPα and MTPβ tended to be significantly higher in the CMD+T3-diet fed rats (Fig. 19).

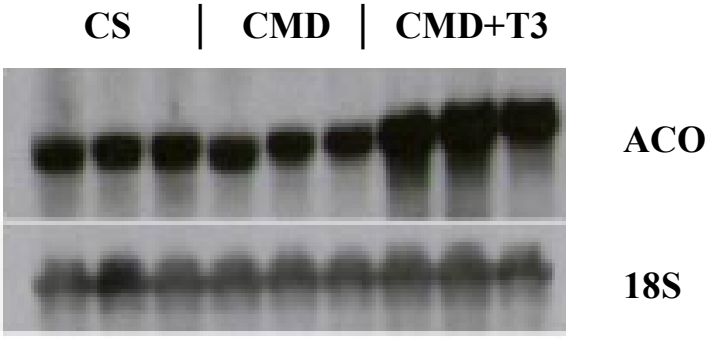

Fig. 18. Northern blot analysis of ACO mRNA levels. Total RNA from the liver of rats fed the CS, CMD or CMD+T3 diet for 1 week was prepared and analyzed as described in ‘‘Materials and Methods’’. 18S was used as a loading control. Each lane represents an individual sample.

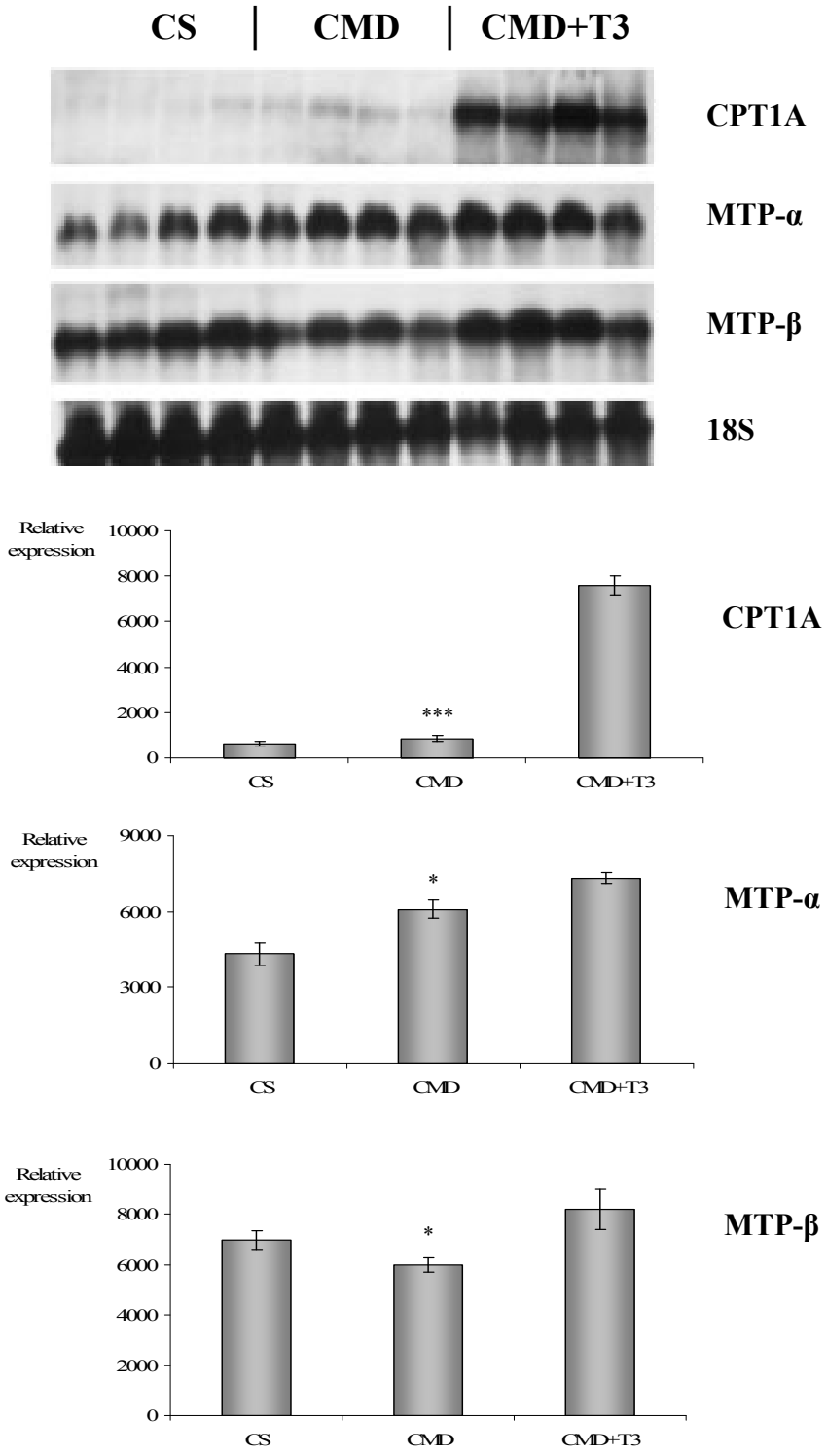

Fig. 19. Northern blot analysis of CPT1A, MTP-α and MTP-β mRNA levels. Total RNA from the liver of rats fed the CS, CMD or CMD+T3 diet for 1 week was prepared and analyzed as described in ‘‘Materials and Methods’’. 18S was used as a loading control. Each lane represents an individual sample. Below, densitometric quantification ($^{***}P<0.001$ or $^{*}P<0.050$ *vs*. CMD+T3).

It is worth mentioning that our results are in line with the general conclusions obtained from studies on 3,5-diiodothyronine (T2), a product of a currently unknown peripheral enzymatic process, most probably utilizing T3 as its precursor, published by Lanni *et al.* in 2005. Their results show that T2 administration to rats receiving a high-fat diet (HFD) (when compared to rats receiving HFD alone) induces a complete disappearance of fat from the liver. This anti-steatotic effect of T2 is accompanied by significant reduction in the body weight, serum triglyceride, cholesterol levels, and an increased hepatic β-oxidation via an activation of the CPT system (Lanni *et al.*, 2005; Moreno *et al.*, 2008). Moreover, in another important study, Nagasawa *et al.* evaluated the effects of bezafibrate, a PPAR pan agonist, on the prevention of steatohepatitis in mice fed the CMD diet. Concurrent administration of the CMD diet and bezafibrate for 5 weeks resulted in reduction in the plasma ALT concentration, hepatic steatosis, products of lipid peroxidation and necro-inflammation. Similar to T3, bezafibrate increased the levels of hepatic mRNAs associated with fatty acid β-oxidation (acyl-CoA oxidase and carnitine palmitoyltransferase-1), but also reduced the levels of cytokines or transcription factors associated with inflammatory process [transforming growth factor-β1 (TGF-β1), IL-6, IL-1β, monocyte chemoattractant protein-1 (MCP-1), tumour necrosis factor α (TNF-α) and nuclear factor κB1 (NF-κB1)] (Nagasawa *et al.*, 2006).

To further clarify the mechanism through which T3 rapidly prevented liver steatosis, we also examined the protein levels of L-FABP.

Alternations in circulating FFAs are widely believed to play a key role in hepatic steatosis. As recently published, members of a conserved family of cytosolic lipid-binding proteins known as fatty acid-binding proteins (FABPs), might contribute to disturbances in lipid homeostasis being involved in the complex and dynamic process of fatty-acid and other lipid trafficking (Chmurzyńska, 2006). Among the numerous functions proposed for FABPs, we can highlight transport facilitation of lipids to specific compartments in the cell, such as to the lipid droplets for storage; to the endoplasmic reticulum for signalling, trafficking and membrane synthesis; to the mitochondria or peroxisome for oxidation; to cytosolic or other enzymes to regulate their activity; and to the nucleus for the control of lipid-mediated transcriptional regulation. Since the discovery of FABPs in the early 1970s, at least 9 members have been identified. The family includes liver (L^-), intestinal (I^-), heart (H^-), adipocyte

(A-), epidermal (E-), ileal (Il-), brain (B-), myelin (M-) and testis (T-) FABPs. However, it should be underlined that no FABP is exclusively specific for a given cell type or tissue, and most tissues express several FABP isoforms (Furuhashi and Hotamisligil, 2008).

The aim of our interest, L-FABP is expressed as an abundant gene product in differentiated enterocytes and hepatocytes, with lower levels of expression in the kidney and colon. Facilitating fatty acid transport and utilization, L-FABP reversibly binds a broad range of ligands, including fatty acids, with a preference for unsaturated *versus* saturated fatty acids, branched-chain fatty acids, cholesterol, and bile acids (Thompson *et al.*, 1999; Storch and Thumser, 2000; Norris and Spector, 2002). In order to enhance the understanding of L-FABP functions and to study its impact on lipid metabolism, mice with a targeted deletion in the L-FABP gene were generated. As reported in the literature, Newberry *et al.* observed significantly less neutral lipid accumulation (~4-fold lower hepatic TG content) in L-FABP$^{-/-}$ mice in comparison to wild-type controls following an acute 48-hour fasting. Moreover, isolated hepatocytes from fasted L-FABP$^{-/-}$ mice demonstrated impaired incorporation of oleate into triglyceride and diacylglycerol (Newberry *et al.*, 2003). It is noteworthy that in the following publication Newberry *et al.* also showed that L-FABP$^{-/-}$ mice placed on a high-saturated fat, high-cholesterol (0,15%) Western diet for up to 18 weeks are less obese and accumulate less hepatic triglyceride than C57BL/6J controls. The main observation of their study was that L-FABP may function as a metabolic sensor in regulating lipid homeostasis and therefore, protecting against Western diet-induced obesity and hepatic steatosis through a series of adaptations in both hepatic and extrahepatic energy substrate use. However, the precise mechanisms remain elusive (Newberry *et al.*, 2006).

Notably, in our experiment, feeding the CMD+T3 diet caused a strong reduction in the levels of L-FABP (Fig. 20). It could suggest that T3 prevents the CMD diet-induced fatty liver by reducing the transfer of fatty acids for glycerolipid biosynthesis.

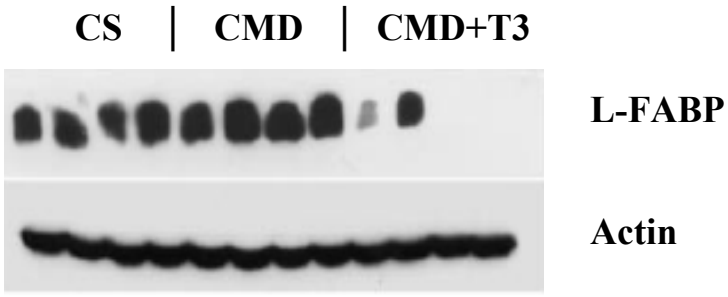

Fig. 20. Changes in protein expression of L-FABP. Western blot analysis was performed as described in ‘‘Materials and Methods’’. Actin was used as loading control.

AIM 1b

Effect of T3 on the reversal of fully established fatty liver

To analyze whether feeding the CMD diet followed by feeding the CMD diet containing T3 could influence the reversal of CMD-induced fatty liver, we followed the **experimental protocol III**. First of all, a significant increase in liver weight and in the liver-to-body weight ratio (Table 5), accompanied by a decrease in serum TG levels and a 4-fold increase in the levels of ALTs was observed in rats fed the CMD-diet compared to animals fed the CS diet (Table 6). By contrast, T3 co-administration provoked a significant reduction in liver weight, liver-to-body weight ratio (Table 5) and serum transaminases (Table 6) compared to rats fed the CMD diet alone. A further decrease in the serum values of TGs was also observed (Table 6).

Treatment	Body Weight (g)	Liver Weight (g)	Liver-to-Body Weight Ratio (%)
CS	270 ± 0.1	9.98 ± 0.2	3.70 ± 0.06
CMD	284 ± 3.7 *	12.08 ± 0.2 ***	4.25 ± 0.07 ***
CMD+T3	255 ± 3.5 $^{\#\#\#}$	8.92 ± 0.2 $^{\#\#\#}$	3.49 ± 0.05 $^{\#\#\#}$

*P<0.05, **P<0.005, ***P<0.001 *vs.* CS

$^{\#}$P<0.05, $^{\#\#}$P<0.005, $^{\#\#\#}$P<0.001 *vs.* CMD

Table 5. Effect of T3 on body weight, liver weight, liver-to-body weight ratio in rats fed the CMD diet for 11 weeks. Values are expressed as means ± SE of 5 to 6 animals per group.

Treatment	TG (mg/dl)	AST (U/L)	ALT (U/L)
CS	282.3 ± 16	147 ± 4.9	43 ± 3.5
CMD	95.8 ± 6.2 ***	211 ± 18 *	179 ± 10 ***
CMD+T3	62.2 ± 4.0 ** ##	157 ± 9.3 #	82 ± 6.8* ###

*P<0.05, **P<0.005, ***P<0.001 *vs.* CS

#P<0.05, ##P<0.005, ###P<0.001 *vs.* CMD

Table 6. Effect of T3 on serum levels of TGs, ALTs and ASTs in rats fed the CMD diet for 11 weeks. Values are expressed as means ± SE of 5 to 6 animals per group.

From a histological point of view, liver sections of the CMD diet-fed rats showed macrovesicular steatosis and numerous fatty droplets within hepatocytes when compared to the CS diet-fed animals. A completely different picture emerged in rats fed the CMD diet with T3. Liver histology showed neither steatosis nor inflammation (Fig. 21). Having noted these changes, we examined whether the histological absence of steatosis in rats fed the CMD diet with T3 could be attributed to altered hepatic triglyceride handling. Determination of the hepatic TG content confirmed that feeding the CMD+T3 diet significantly lowered total hepatic triglyceride levels compared to the CMD diet-fed rats (Fig. 22).

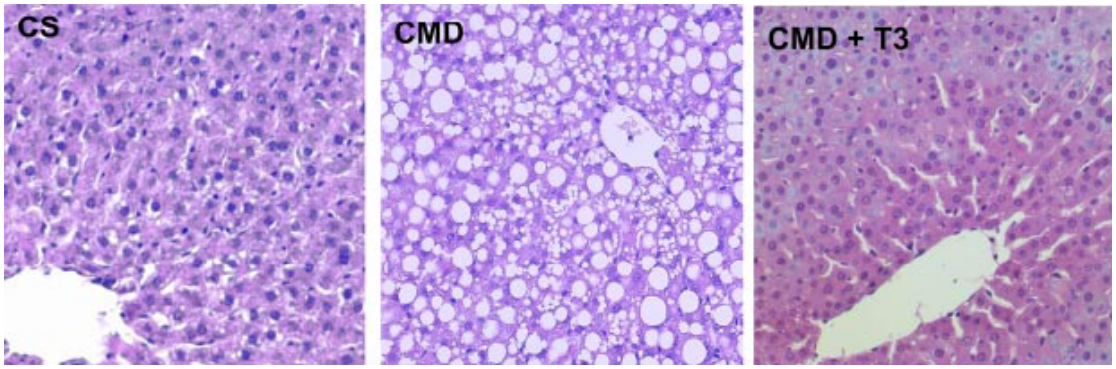

Fig. 21. Photomicrographs showing hematoxylin-eosin stained sections of liver tissue from rats fed the CS or CMD diet for 11 weeks or CMD diet for 10 weeks followed by 1 week of T3 co-feeding. Numerous fatty droplets within hepatocytes were observed in the liver from rats fed the CMD diet (original magnification x20).

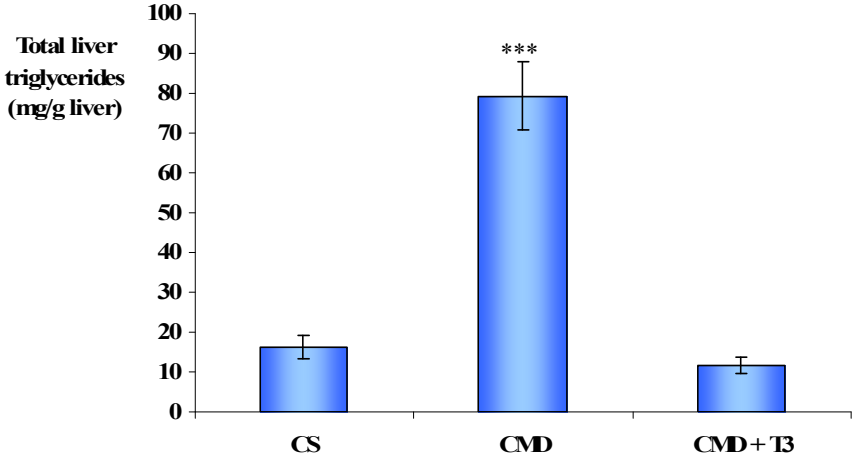

Fig. 22. Hepatic triglyceride content. Data is presented as means ± SE; 5 rats per group. $^{***}P<0.001$ *vs.* CMD+T3 and CS. Difference between CS and CMD+T3 is not significant.

Recently, the group of Ip *et al.*, after having previously shown that co-administration of the peroxisome proliferator-activated receptor α (PPARα) agonist, Wy-14,643, prevents the development of CMD diet-induced steatohepatitis, have tested whether this compound ameliorates established steatohepatitis. In accordance with our results, treatment with this fibrate significantly decreased ALT levels and reduced fat accumulation. They have also found that the reversal of CMD diet-induced hepatic inflammation was accompanied by the reduction of the number and activation of

hepatic macrophages, down-regulation of hepatic vascular cell adhesion molecule-1 (VCAM-1) and intercellular adhesion molecule-1 (ICAM-1) mRNA levels, downstream targets of nuclear factor κB (NF-κB) activation (Ip *et al.*, 2003; Ip *et al.*, 2004). Therefore, there is a considerable interest in delineating the factors that initiate the onset of necro-inflammation. It is known that lipoperoxides are not only increased in areas of hepatic steatosis in human NASH but also accumulate in the livers of animals fed the CMD diet (Seki *et al.*, 2002). Some of the end products of lipid peroxidation have proinflammatory properties and may play a crucial role in the pathogenesis of steatohepatitis mediating inflammatory recruitment directly [e.g. it was found that 4-hydroxy-2-nonenal (4-HNE), the end product of lipid peroxidation, represents one of the inducers of COX-2 (Kumagai *et al.*, 2000)] or indirectly by activating NF-κB with downstream consequences that include expression of adhesion molecules, cytokines (TNF-α, IL-1β, IL-6) and COX-2 (Leclercq *et al.*, 2004; Yu *et al.*, 2006).

The cyclooxygenase (COX) enzyme (termed also prostaglandin H synthase) is known to catalyze the first step of the synthesis of prostanoids (including prostaglandins, thromboxanes, prostacyclins) by converting arachidonic acid into prostaglandin H_2. In detail, COX is a bifunctional enzyme exhibiting both fatty acid COX activity (catalyzing the conversion of arachidonic acid to prostaglandin G_2) and prostaglandin hydroperoxidase activity (catalyzing the conversion of prostaglandin G_2 to prostaglandin H_2). In the early 1990s, two distinct isoforms of COX were recognized. COX-1 is constitutively expressed as a ‘‘housekeeping’’ enzyme in most tissues and mediates physiological responses, including cytoprotection of the stomach and platelet aggregation. By contrast, COX-2, primarily responsible for the synthesis of the prostanoids involved in pathological processes (acute and chronic inflammatory states), is present in very low amounts and becomes rapidly induced by lipid peroxides, oxidative stress, NF-κB, cytokines (TNF-α, IL-1β, IL-6), and TGF-β1 (Hinz and Brune, 2002). Recently, Yu *et al.* have reported that the temporal profile of increased COX-2 expression in male C57BL/6N mice fed the CMD diet for five weeks paralleled the histological development of steatohepatitis. COX-2 up-regulation was preceded by activation of NF-κB and coincided with significantly elevated levels of TNF-α, IL-6 and ICAM-1. However, induction of COX-2, proposed as a pro-inflammatory mediator in steatohepatitis, resulted completely suppressed by dietary supplementation with the potent and specific PPAR-α agonist, Wy-14,643 (Yu *et al.*, 2006). For this reason, we made an attempt to investigate the effect of T3 on COX-2 protein levels. The results

shown in Figure 23 demonstrate that COX-2 protein expression is increased in the CMD diet-fed animals when compared to the CS diet-fed rats, whereas the CMD+T3 diet-fed animals have the hepatic levels of this pro-inflammatory mediator strongly decreased.

Strikingly up-regulated activity of cytochrome P450 (CYP) enzyme 2E1 has been documented as another important event promoting liver injury in a rat dietary model of steatohepatitis (Weltman *et al.*, 1998). As proposed by Liu *et al.*, CYP2E1-overexpressing hepatocytes have both basal and TNF-α-induced increased levels of c-Jun N-terminal kinase (JNK) activity (Liu *et al.*, 2002). Members of the JNK family, also called stress-activated protein kinase (SAPK), subgroup of mitogen-activated protein kinases (MAP kinases), involved in proliferation, apoptosis, motility, metabolism and DNA repair, are known to be activated by diverse extracellular stimuli, including UV irradiation, pro-inflammatory cytokines and certain mitogens. Phosphorylation on invariant threonine and tyrosine residues, within a TXY motif in the activation loop, by dual specificity MAP kinase kinases (MAPKKs) is required for all MAP kinases activation (Minden *et al.*, 1997). Dysregulated JNK signalling has been implicated in many diseases involving neurodegeneration, chronic inflammation, birth defects, cancer and ischemia/reperfusion injury (Johnson and Nakamura, 2007). Moreover, it has been reported that suppression of the JNK pathway in the liver decreases insulin resistance and markedly improves glucose tolerance in two different diabetic animal models (Nakatani *et al.*, 2004). In the CMD diet-fed mice, activation of hepatic JNK, c-Jun, and AP-1 signalling occurs in parallel with the development of steatohepatitis (Schattenberg *et al.*, 2006); therefore, the levels of active, phosphorylated JNK (phospho-SAPK/JNK) were examined in our experimental model of steatohepatitis. While very low activation of SAPK/JNK was observed in the non-injured livers of CS diet-fed animals, increased levels of phosphorylated JNK were detected in CMD diet-fed animals. Co-feeding with T3 almost completely inhibited activation of this kinase (Fig. 23).

Successively, we examined the effect of T3 on the hepatic levels of phosphorylated STAT 3, a member of the Janus kinase-signal transducers and activators of transcription (JAK-STAT) signalling pathway implicated in a bewildering complexity of cellular responses to cytokines and growth factors in the hematopoietic, immune, neuronal and hepatic systems (Turkson and Jove, 2000). In the liver, STAT 3, mainly activated by IL-6 and its related cytokines (e.g. oncostatin M, cardiotrophin-1), and IL-22 plays a crucial role in the acute phase response, promotion of liver regeneration, inflammation,

glucose homeostasis, and hepatic lipid metabolism (Gao, 2005). STAT 3 has a conserved amino-terminal domain mediating the interaction between two STAT dimers to form a tetramer, a coiled-coil domain involved in interactions with regulatory proteins and other transcription factors, a DNA-binding domain making direct contact with STAT-binding sites in gene promoters, an SH2 domain required for STAT dimerization, and a carboxy-terminal transactivation domain; similarly to other STAT-family members (Levy and Lee, 2002). This transcription factor is activated by tyrosine phosphorylation at a Tyr705, as well as by serine phosphorylation in the carboxy-terminal transcriptional activation domain (Ser727). Tyrosine phosphorylation in response to cytokine stimulation is mediated by a Janus kinase (most often JAK1) and activates SH2-mediated dimerization rapidly followed by nuclear translocation. STAT 3 dimers bind to interferon-γ-activated sequence (GAS) DNA element resulting in the transcriptional regulation of a wide range of target genes, such as: c-jun, c-myc, Jun B, cyclin D1, $p21^{WAF1/Cip1}$, and acute-phase genes (Darnell Jr. *et al.*, 1994; Gao, 2005). STAT 3 serine phosphorylation enhances its transcriptional activity and is required for maximal activation of its signalling (Turkson and Jove, 2000). Our studies have clearly shown that STAT 3 activation was significantly up-regulated in the liver of the CMD diet-fed animals compared to the CS diet-fed rats. In accordance with its suggested proinflammatory role (Suzuki *et al.*, 2001; Lovato *et al.*, 2003; Han *et al.*, 2005; Mudter *et al.*, 2005), hepatic protein levels of phosphorylated STAT 3 were strongly reduced in the livers of rats given the CMD+T3 diet, compared to the CMD diet-fed animals (Fig. 23).

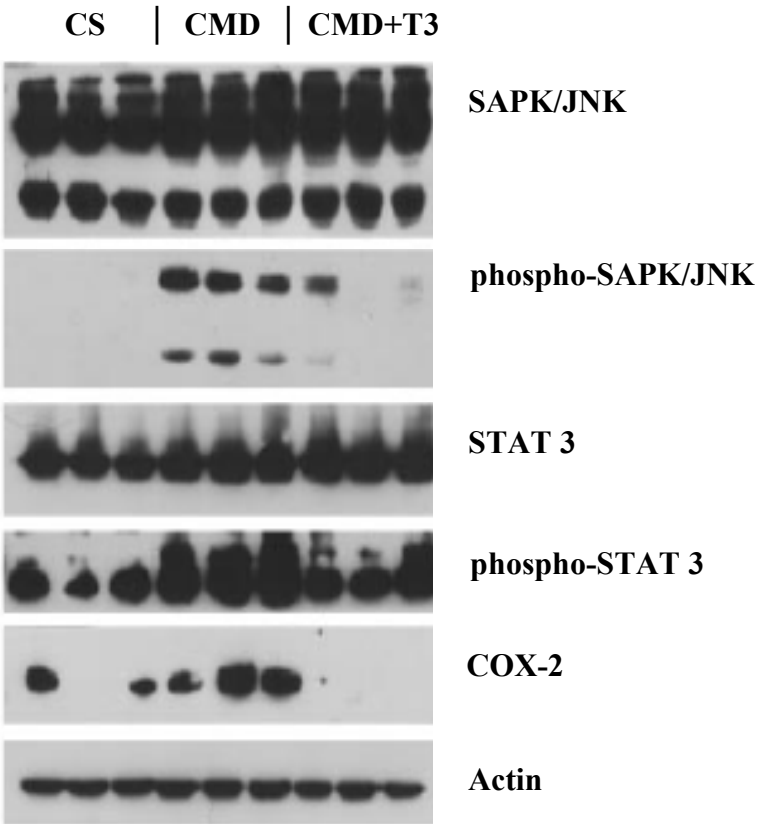

Fig. 23. Hepatic SAPK/JNK, phospho-SAPK/JNK, STAT 3, phospho-STAT 3 and COX-2 protein levels determined by Western blot analysis (performed as described in ‘‘Materials and Methods’’). Actin was used as a loading control. Each lane represents a single sample.

AIM 2a

Effect of GC-1 on the prevention of CMD-induced fatty liver

In our experiments, we saw that an excess of triiodothyronine can result in therapeutically desirable effects. At the same time, T3 is known to increase heart rate, speed and force of systolic contraction, shorten the duration of diastolic relaxation and affect vascular tone (Trost *et al.*, 2000). Therefore, the primary aim of this experiment was to investigate if the beneficial effect of T3 on liver steatosis and steatohepatitis might be achieved by GC-1, a TRβ-selective agonist, administration without inducing a thyrotoxic state.

Consequently, we used the **experimental protocol IV**. Rats were fed the CS, CMD or CMD diet supplemented with 5 mg/kg of GC-1 for 2 weeks. In all experimental groups, no differences in physical activity and behaviour were observed. Moreover, appearance of animals remained healthy. Similar to the effect of T3, co-administration of GC-1 for 2 weeks provoked significant weight loss, reduced liver-to-body weight ratio and serum TG levels (Table 7, 8). As expected, within 14 days of CMD+GC-1 exposure, serum levels of ALTs and ASTs were also diminished (Table 8).

Treatment	Body Weight (g)	Liver Weight (g)	Liver-to-Body Weight Ratio (%)
CS	155 ± 2.9	7.28 ± 0.17	4.69 ± 0.04
CMD	149 ± 3.3	11.42 ± 0.36 ***	7.66 ± 0.16 ***
CMD+GC-1	136 ± 2.5 $^{**\,\#}$	6.83 ± 0.30 $^{\#\#\#}$	5.02 ± 0.21 $^{\#\#\#}$

*P<0.05, **P<0.005, ***P<0.001 *vs.* CS

$^{\#}$P<0.05, $^{\#\#}$P<0.01, $^{\#\#\#}$P<0.001 *vs.* CMD

Table 7. Effect of GC-1 on body weight, liver weight, liver-to-body weight ratio in rats fed the CMD diet for 2 weeks. Values are expressed as means ± SE of 5 to 6 animals per group.

Treatment	TG (mg/dl)	AST (U/L)	ALT (U/L)
CS	162 ± 13	73 ± 4	124 ± 6
CMD	85 ± 10 ***	174 ± 17 **	197 ± 12 **
CMD+GC-1	53 ± 3 *** #	134 ± 10 * #	168 ± 9 * #

*P<0.05, **P<0.005, ***P<0.001 *vs.* CS

#P<0.05, ##P<0.01, ###P<0.001 *vs.* CMD

Table 8. Effect of GC-1 on serum levels of TGs, ALTs and ASTs in rats fed the CMD diet for 2 weeks. Values are expressed as means ± SE of 5 to 6 animals per group.

Furthermore, CMD diet-fed rats developed macrovesicular steatosis, whereas in the CMD+GC-1 group histological analysis revealed minimal steatosis. No steatosis was observed in *zone 1* and *2* of the liver acinus except the periportal areas where lipid droplets were still present (Fig. 24). To further validate histological differences in the presence of steatosis, hepatic triglyceride content was determined (Fig. 25). Similar to T3, GC-1 caused a reduction of the CMD-induced TG accumulation in the liver. However, TRβ-selective agonist exerted a weaker effect than T3 in reduction of hepatic TG content.

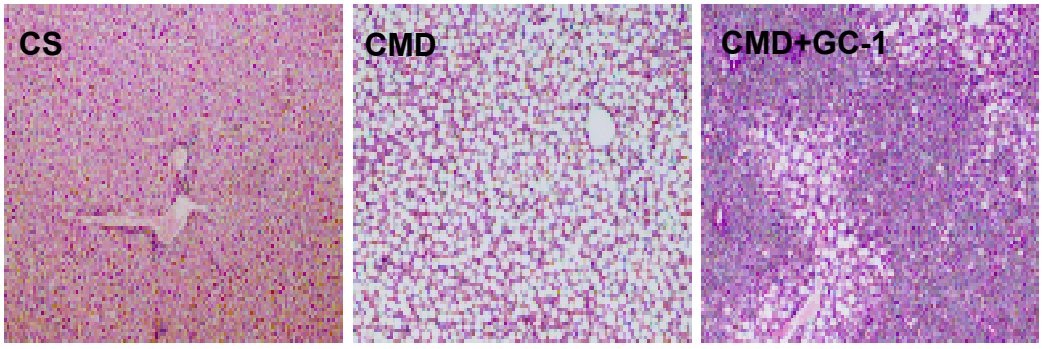

Fig. 24. Representative histology of liver tissue. Hematoxylin-eosin staining of liver sections from rats fed the CS, CMD and CMD+GC-1 diet for 2 weeks (original magnification x20).

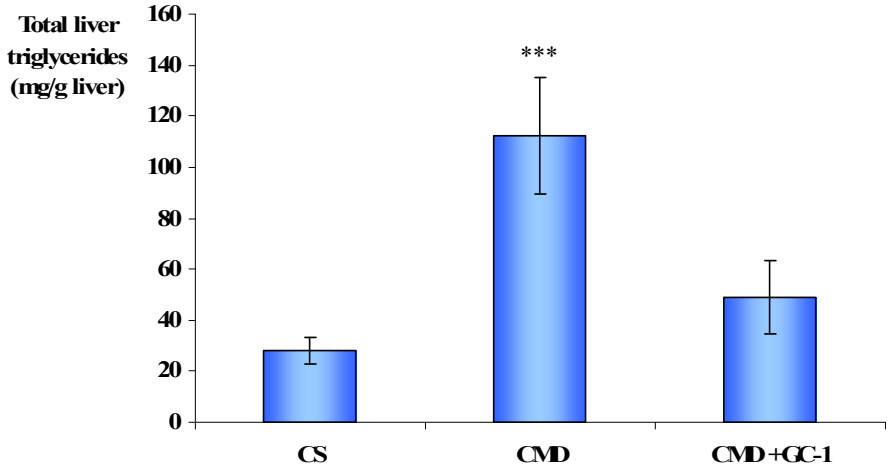

Fig. 25. Hepatic triglyceride content. Values are expressed as means ± SE; 5 rats per group. $^{***}P<0.001$ *vs.* CMD+GC-1 and CS. Difference between CS and CMD+GC-1 is not significant.

A satisfactory unifying mechanism explaining the causes leading to steatohepatitis has been sought for many years. The most frequently posed question was why some patients with steatosis, regardless of etiology, never develop progressive liver disease. An enormous number of reports in the literature led to the identification of oxidative stress as a factor involved in the pathogenesis of steatosis and steatohepatitis. A milestone, which provided a pathophysiologic rationale for the progression of NAFLD, was the ‘‘two-hit’’ theory launched by Day and James in 1998. According to this model (Fig. 26), the initial insult or ‘‘first hit’’ is represented by hepatic steatosis, a prerequisite for subsequent events that lead to liver injury. Liver becomes susceptible to secondary insults, however, the disease does not progress unless additional cellular events occur. The presence of some other factor(s)-‘‘second hit’’ is required for the development of steatohepatitis. The ‘‘second hit’’, stated as a central biochemical mechanism of hepatocellular injury in NASH, can be represented by free radicals capable of inducing imbalance between pro-oxidant and antioxidant chemical species (oxidative stress) (Day and James, 1998).

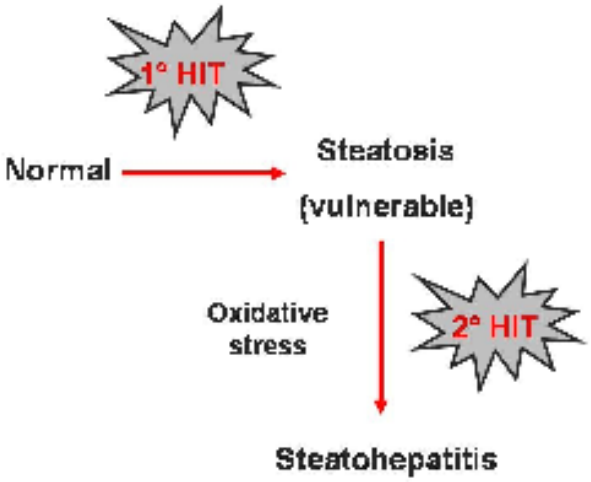

Fig. 26. The ‘‘two hit’’ hypothesis for the pathogenesis of non-alcoholic steatohepatitis (Koteish and Diehl, 2002).

In the physiological state cytochrome P450, peroxisomal β-oxidation and mitochondrial electron leak are 3 possible sites at which pro-oxidant ROS can be generated. In particular, strikingly up-regulated activity of cytochrome P450 (CYP) enzyme 2E1, known to form active oxygen species (superoxide anions, hydroxyl radicals, hydrogen peroxides) during microsomal ω-oxidation, has been documented in the fatty liver (Weltman *et al.*, 1998; Robertson *et al.*, 2001). There is also accumulating evidence that in an environment enriched with lipids, mitochondrial dysfunction (hampering electron transfer within the respiratory chain) lead to an overproduction of ROS (Kass, 2006; Serviddio *et al.*, 2007).

A consequence of significantly increased ROS generation includes damage of membranes via lipid peroxidation. The process of lipid peroxidation, leading to oxidative destruction of polyunsaturated fatty acids (PUFAs), integral of cellular membranes, is initiated by the attack on a fatty acid or fatty acyl side chain of any chemical species having sufficient reactivity to abstract a hydrogen atom from a methylene carbon in the side chain. In living cells, reactive oxygen species (such as OH·) have the potential to cause initiation of lipid peroxidation. The greater the number of double bonds in a fatty acid side chain, the easier is the removal of a hydrogen atom. Therefore, PUFAs are readily attacked by free radicals and particularly susceptible to peroxidation. The hydrogen atom has a single electron and its removal leaves behind an unpaired electron on the carbon atom to which it was originally attached. The resulting fatty acid radical usually undergoes molecular rearrangement, followed by reaction with

molecular oxygen creating a peroxyl radical. Then, peroxyl radicals can react with each other propagating the chain reaction of lipid peroxidation or abstract hydrogen from adjacent fatty acid side chains producing a lipid hydroperoxide (Halliwell and Chirico, 1993). Lipid hydroperoxides breakdown in biological systems forms a great diversity of aldehydes. The most abundant are malondialdehyde (MDA) and 4-hydroxyalkenals (4-HDA), in particular 4-hydroxy-2-nonenal (4-HNE) (Esterbauer and Cheeseman, 1990).
First of all, lipid peroxidation products can damage the mitochondrial genome, which is particularly prone to oxidative stress. Although nuclear DNA encodes most respiratory chain polypeptides, 13 polypeptides are encoded by mitochondrial DNA (mtDNA). Thus, mtDNA damage can secondarily impair electron transfer in the respiratory chain. Secondly, some lipid peroxidation products are potent inducers of mitochondrial permeability transition (MPT) that can lead to cell death (Begriche *et al.*, 2006). Lastly, reactive lipid peroxidation products have the potential to diffuse from their site of origin to reach distant intracellular and extracellular targets, thereby amplifying the oxidative stress that led to their initial formation (Neuschwander-Tetri *et al.*, 2003b; Browning and Horton, 2004). In addition, the aldehyde products, 4-hydroxyalkenals and malondialdehyde (MDA), are known to be capable of activating hepatic stellate cells and contribute to inflammation by activating NF-κB. This transcription factor regulates the expression of several proinflammatory cytokines and adhesion molecules (TNF-α, IL-8, E-selectin) (Diehl *et al.*, 2005; Choi and Diehl, 2008).
The CMD-diet model is recognised as a very reproducible pattern of lipid peroxidation in the liver and offers a perspective in the exploration of the role of free radicals in fat accumulation. Accumulating evidence that oxidative stress and lipid peroxidation are the most pathogenic mechanisms of non-alcoholic fatty liver disease, led us to examine this issue.
To avoid misleading results, great importance on the reliable assessment of lipid peroxidation should be placed (Esterbauer *et al.*, 1991). Even if many assays are available to measure lipid peroxidation, determination of the sum of malondialdehyde and 4-hydroxyalkenals has been widely used as a convenient indicator of lipid peroxidation (Esterbauer and Cheeseman, 1990). For this purpose, the TBA (tiobarbituric acid) test, probably because of its simplicity and cheapness, is one of the most commonly applied assays. In the sample under test one molecule of MDA reacts with two molecules of TBA with the production of a pink chromogen having an absorption maximum at 532-535 nm (Janero, 1990). However, it is well documented

that the TBA test application to body fluids and tissue extracts can produce a host of problems. First, this test is intrinsically nonspecific for MDA and aldehydes other than MDA can form chromogens with absorbance at 532 nm. Second, it rarely measures the free MDA content of the lipid system. Most, if not all, of the MDA measured is generated by decomposition of lipid peroxides during the acid heating stage of the test. Third, peroxide decomposition produces radicals that can start peroxidation of other lipid molecules during the assay, amplifying the response. In conclusion, the TBA assay is strongly influenced by the reaction conditions (Halliwell and Chirico, 1993).

As a consequence, for our study, we used a colorimetric assay for lipid peroxidation developed by Gérard-Monnier *et al.* in 1998. The Bioxytech® LPO-586 kit™ is based on the reaction of a chromogenic reagent, N-methyl-2-phenylindole, with MDA and 4-HDA. Under mild-temperature conditions, using a methanesulfonic acid-based medium, one molecule of either MDA or 4-HDA reacts with 2 molecules of N-methyl-2-phenylindole, to yield a stable chromophore with intense maximal absorbance at 586 nm.

In this experiment, measurement of hepatic lipoperoxides revealed that in the CMD diet-fed rats lipid peroxidation was increased compared to those fed the control diet. It was important to note that administration of the CMD diet with GC-1 significantly diminished lipoperoxidation compared to rats fed the CMD diet alone (Fig. 27).

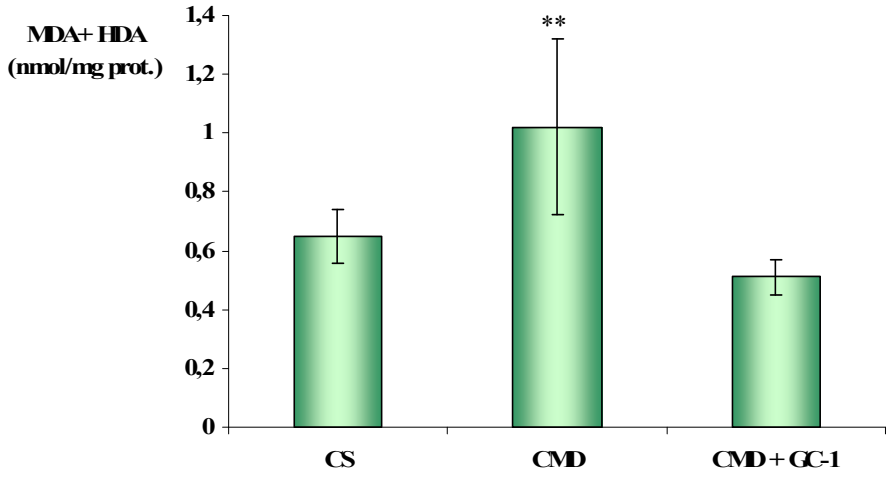

Fig. 27. Histogram demonstrating LPO levels. $^{**}P<0.01$ *vs*. CMD+GC-1 and CS. Difference between CS and CMD+GC-1 groups is not significant.

AIM 2b

Effect of GC-1 on the reversal of fully established fatty liver

The final experiment was performed to investigate if the severity of fully established fatty change could be reverted by feeding the CMD diet containing GC-1. To examine this potential capacity of GC-1 we followed the **experimental protocol V**. As expected, a significant increase in liver weight and in the liver-to-body weight ratio was observed in rats fed the CMD-diet (Table 9). This coincided with a decrease in serum TG levels and an increase in the levels of ALTs and ASTs (Table 10). GC-1 co-administration caused a decrease in both liver weight and liver-to-body weight ratio and a decrease in the serum values of TGs compared to rats fed the CMD diet alone (Table 9, 10). The significant reduction of AST and ALT levels was also observed in the CMD+GC-1 diet-fed rats (Table 10).

Histological analyses of liver sections confirmed that rats fed the CMD diet for 12 weeks developed severe macrovesicular steatosis. Successively, the fat pattern was observed in the CMD+GC-1 diet-fed animals for 14 days, following a 10-week CMD diet feeding. In addition, while the CMD+GC-1 feeding, 3- and 7-day intermediate time points were added in order to be able to observe the preceding effect of the 14-day treatment. Representative photomicrographs of hematoxylin-eosin-stained liver sections (Fig. 28) show that after only 3 days of treatment, GC-1 co-feeding caused a reduction in hepatic steatosis. This effect was even more evident after 7 days of treatment and almost complete disappearance of hepatic steatosis (very few small droplets were present) after 14 days was observed (Fig. 28). Consistent with the histological findings, 7- and 14-day treatment with CMD+GC-1 significantly ($P<0.001$) reduced hepatic triglyceride content compared to CMD diet-fed rats (Fig. 29). To assess the impact of GC-1, hepatic lipoperoxide levels were measured. As expected, the disappearance of hepatic TGs was accompanied by a concomitant decrease of MDA and 4-HDA levels (Fig. 30).

Treatment	Body Weight (g)	Liver Weight (g)	Liver-to-Body Weight Ratio (%)
CS	297 ± 6.7	10.63 ± 0.27	3.58 ± 0.07
CMD	282 ± 1.2	15.05 ± 0.13 ***	5.34 ± 0.03 ***
CMD+GC-1	255 ± 4.8 *** ##	9.20 ± 0.36 ###	3.60 ± 0.08 ###

*P<0.05, **P<0.005, ***P<0.001 *vs.* CS
#P<0.05, ##P<0.01, ###P<0.001 *vs.* CMD

Table 9. Effect of GC-1 on body weight, liver weight, liver-to-body weight ratio in rats fed the CMD diet for 12 weeks. Values are expressed as means ± SE of 5 to 6 animals per group.

Treatment	TG (mg/dl)	AST (U/L)	ALT (U/L)
CS	204 ± 25	34 ± 6	43 ± 5
CMD	36 ± 2 ***	279 ± 11 ***	248 ± 13 ***
CMD+GC-1	47 ± 2 ###	159 ± 11 *** ##	194 ± 13 * #

*P<0.05, **P<0.005, ***P<0.001 *vs.* CS
#P<0.05, ##P<0.01, ###P<0.001 *vs.* CMD

Table 10. Effect of GC-1 on serum levels of TGs, ALTs and ASTs in rats fed the CMD diet for 12 weeks. Values are expressed as means ± SE of 5 to 6 animals per group.

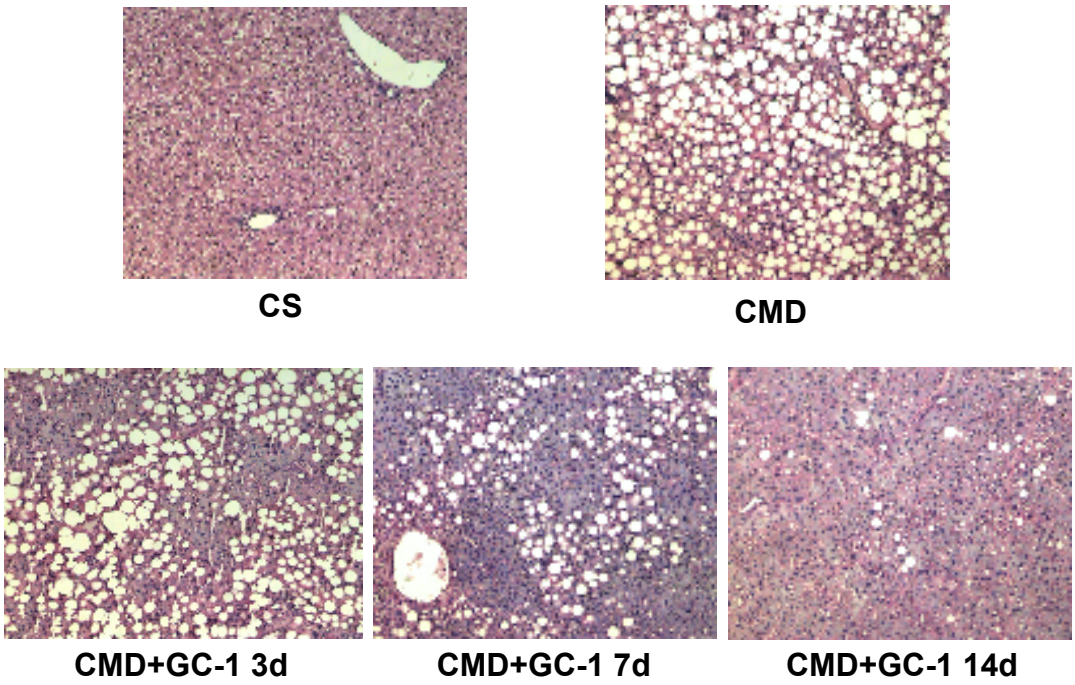

Fig. 28. Representative histology of liver tissue. Hematoxylin-eosin stained liver sections from rats fed the CS or CMD diet for 12 weeks or CMD diet for 10 weeks followed by 3, 7, and 14 days of CMD+GC-1 co-feeding (original magnification x20).

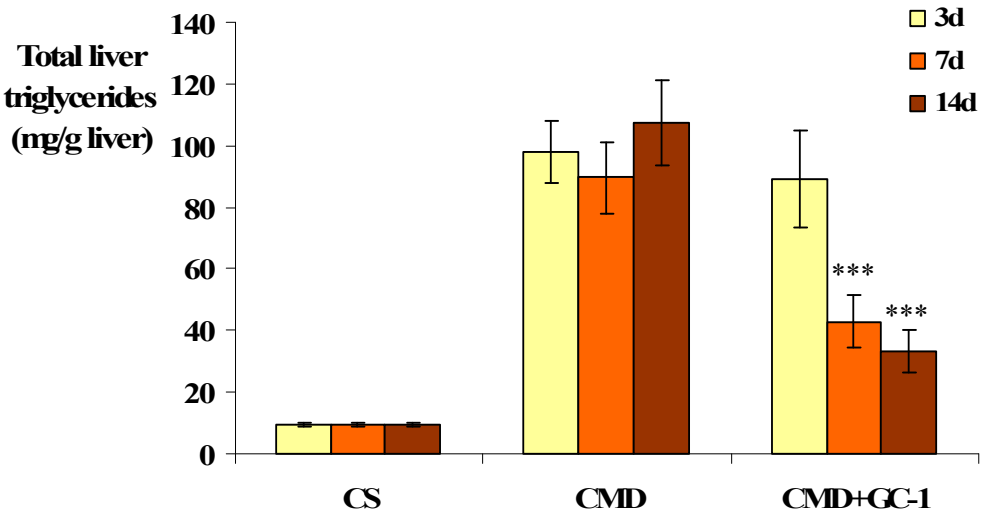

Fig. 29. Hepatic triglyceride content. Data is expressed as means ± SE; 5 rats per group. $^{***}P<0.001$ *vs*. CMD.

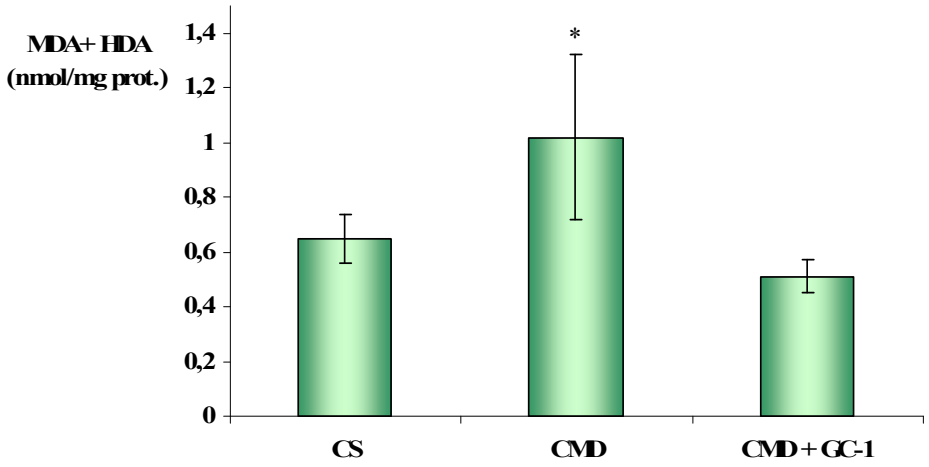

Fig. 30. Hepatic lipoperoxide levels. $^{*}P<0.05$ *vs*. CMD+GC-1 and CS.

AIM 3

Application of a metabolomic technique in order to analyse the liver lipid profile changes during treatment with GC-1

Metabolites are known to be involved as key regulators of systems homeostasis (Mattila *et al.*, 2008). Metabolic profiling (metabolomics), developed to an accepted and valuable tool in life sciences, is the measurement in biological systems of the complement of low-molecular-weight metabolites and their intermediates that reflects the dynamic response to genetic modification and physiological, pathophysiological, and/or developmental stimuli (Nicholson *et al.*, 1999; Clarke and Haselden, 2008). In analogy to the genome, which is used as synonym for the entirety of all genetic information, the metabolome represents the entirety of the metabolites within a biological system (Oldiges *et al.*, 2007).

In recent years, lipidomics or lipid profiling (an extension of metabolomics), which measures the lipid complement of a cell, tissue or organism, has caught scientists' attention as a research tool and become an important target of the postgenomic revolution (Roberts *et al.*, 2008). The importance of the lipidomic analysis is considerable, knowing that, the disruption of lipid metabolic pathways accompanies many pathological states (e.g. cancer, diabetes, as well as neurodegenerative and infectious diseases) (Yetukuri *et al.*, 2007). The rapid development in the areas of mass spectrometry (MS) and chromatography have led to significant advances within the field of lipidomics and liquid chromatography (LC)-MS has increasingly occupied an important position in the lipidomic methodologies (Plumb *et al.*, 2003; Villas-Bôas *et al.*, 2005; Roberts *et al.*, 2008). This powerful technique combines the physical separation capabilities of LC with the mass analysis capabilities of MS. Unlike gas chromatography (GC)-MS, LC-MS seems to be a more versatile analytical method as it covers much wider mass range and does not require derivatization (Xie *et al.*, 2008). Recently, a technique defined as ultra-performance liquid chromatography-mass spectrometry (UPLC-MS) has risen as a new category of analytical separation representing an improvement in chromatographic performance due to the evolution of packing materials used to effect the separation. According to the Van Deemter equation, which is particularly important in column design, as the particle size decreases to less

than 2.5 µm, there is a significant gain in chromatographic efficiency. Therefore, the use of sub-2 µm particles in UPLC, while reducing run times, improved the peak capacity (maximal number of resolved peaks that fit in a chromatogram), resulting in greater differentiation among peaks, as well as sensitivity because chromatographic bands appear more concentrated and elute as sharper peaks (Swartz, 2005). Coupled to quadrupole time-of-flight mass spectrometry (QTOF-MS) which delivers accurate mass identification, UPLC-QTOF-MS is increasingly being used for reliable lipid profiling (Beattie *et al.*, 2005).

Therefore, for our study, we employed the UPLC-QTOF-MS technique to observe major changes in the liver lipid profile. This metabolomic approach was applied to rats fed the CS or CMD diet for 12 weeks or CMD diet for 10 weeks followed by 3, 7, and 14 days of CMD+GC-1 co-feeding (see the **experimental protocol V**). Moreover, the fourth group of rats fed rodent standard diet (a nutritionally balanced diet based on the growth criteria of the utilized species, on the contrary of the hyperlipidic CS diet) for 12 weeks was added.

Retention time (the time between sample injection and an analyte peak reaching a detector at the end of the column) and mass-to-charge ratio (*m/z)* data pairs used as the identifier of each detected peak from UPLC-QTOF-MS analysis were pre-processed and aligned employing XCMS, as shown in Figure 31.

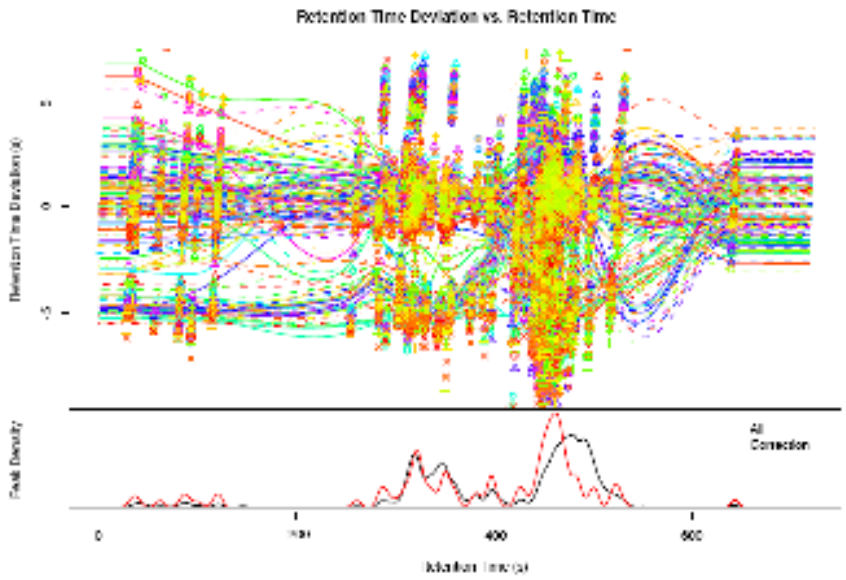

Fig. 31. Chromatographic alignment (XCMS). Sample profiles are coloured using a rainbow based on the order in which they were run, with red first and violet last.

The resulting matrix of retention corrected peak groups was further exported into SIMCA-P software for multivariate statistical analysis. Application of multivariate analysis to UPLC-MS data, pioneered by Nicholson *et al.* in 1999, facilitated accurate discrimination of the experimental groups. It should be mentioned that pattern recognition techniques are divided into unsupervised approaches where class membership is not known (e.g. principal components analysis-PCA), and supervised approaches where class membership is used to maximise the separation of data into distinct clusters (e.g. Partial Least Squares-Discriminant Analysis-PLS-DA) (Griffin, 2006a, b). In our study, we employed both PCA and PLS-DA pattern recognition.

To achieve the natural interrelationship including clustering and outliers without *a priori* knowledge of the data set, we applied PCA. As evident from Figure 32, the PCA scores plot exhibited a clear clustering of 3 distinct groups of rats fed the CMD, CMD+GC-1 and CS/standard diet. Additionally, the supervised PLS-DA model generated a more perfect differentiation ability among these 3 groups. The explained variation (R^2) and predicted variation (Q^2) helped to evaluate the quality of both models, indicating their reliability. To further improve this separation, PLS-DA pattern recognition was applied to the spectral data set only from tissue extracts of CS and standard-diet fed animals demonstrating differences in the lipid profile in these two groups. PLS-DA scores plot recapitulated in Figure 33 shows an apparent clustering of 2 distinct groups of rats fed the CS or standard diet.

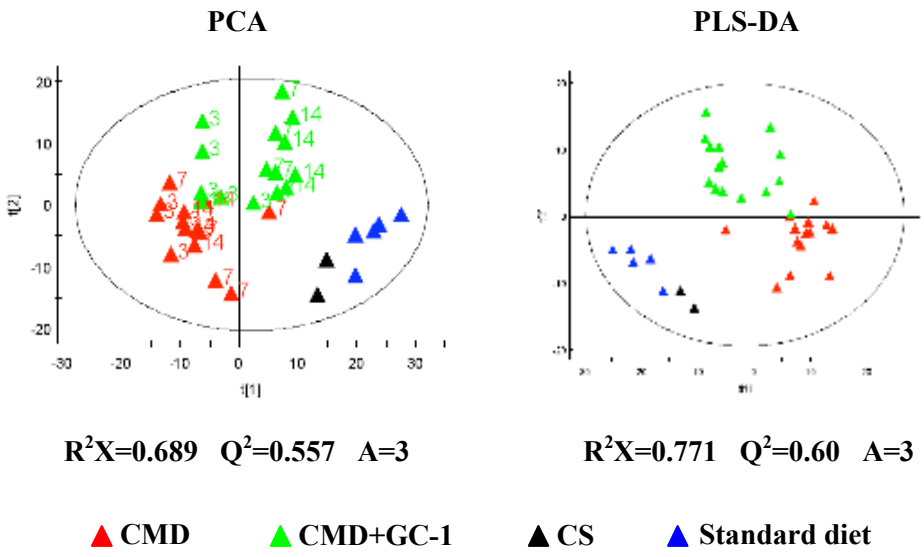

Fig. 32. Resulting PCA and PLS-DA scores plot from UPLC-QTOF-MS data sets. The quality of the models was evaluated with the relevant R^2 and Q^2.

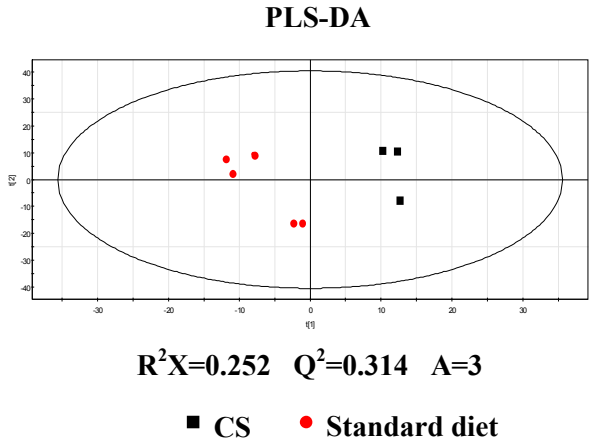

Fig. 33. PLS-DA scores plot from UPLC-QTOF-MS data sets. The quality of the model was evaluated with the relevant R^2 and Q^2.

Successively, metabolomics analysis allowed us to monitor the metabolite comparison between the CMD and CMD+GC-1 diet-fed animals. As demonstrated in Figure 34, the PCA scores plot of the CMD+GC-1- and CMD diet-fed rats suggests that the lipid content after 3 days of CMD+GC-1 treatment is similar to that of the CMD diet-fed animals and requires 7 to 14 days to stabilize. The quality of the model assessed with the relevant R^2 and Q^2 results good. Therefore, metabolomic analyses result consistent with previously discussed biochemical triglyceride measurement (Fig. 35).

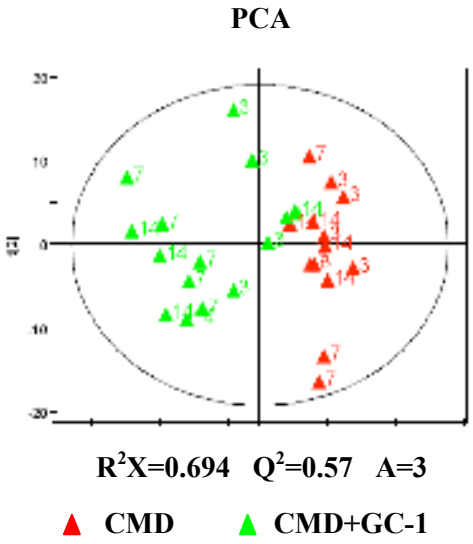

Fig. 34. Resulting PCA scores plot from UPLC-QTOF-MS data sets. The quality of the model was evaluated with the relevant R^2 and Q^2.

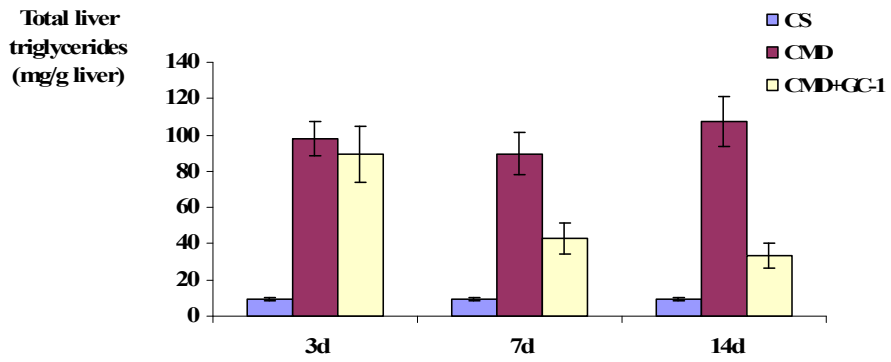

Fig. 35. Liver triglyceride content in rats fed the CS or CMD diet for 12 weeks or CMD diet for 10 weeks followed by 3, 7, and 14 days of CMD+GC-1 co-feeding.

In summary, the highly sensitive technique UPLC-QTOF-MS facilitates the achievement of an accurate picture of the changes in the lipid profile of the liver. The UPLC-QTOF-MS-based methodology went deeper than the histological and biochemical examinations, giving a clear evidence that CS and CMD+GC-1 (despite the absence of fat accumulation) lipid profiles are not superimposed. Moreover, a major advantage of the UPLC-MS technique is the ability to separate lipids from complex biological fluids into individual lipid categories (fatty acyls, glycerolipids, glycerophospholipids, sphingolipids, sterol lipids, prenol lipids, saccharolipids, polyketides) and/or within the same category into distinct classes and subclasses, which successively can be identified by searching spectral databases (Fahy *et al.*, 2005). Although, in our study, we did not take advantage of this possibility, this approach may allow a comprehensive analysis of lipid molecules and further elucidate differences in the lipid profile. Taking into consideration the complexity of lipid categories, this analytical method affords screening of many lipid molecular species surpassing traditional lipid biochemistry. For example, in a recent study by Yetukuri *et al.*, the UPLC-MS-based lipodomic characterisation of the fatty liver of the genetically obese insulin resistant ob/ob mice showed increased deposition of short chain tri- and di-acylgycerol species and diacylphosphoglycerols associated with proportional increase of reactive ceramide lipid species, as well as down-regulation of sphingomyelins, the substrate for ceramide synthesis (Yetukuri *et al.*, 2007).

Finally, another important challenge in the metabolomic area is related to the future studies in identifying specific changes (biomarkers) in lipid composition at very early

stages of hepatic steatosis using the plasma. The metabolomic approach could also lead to the development of non-invasive techniques in order to replace liver biopsy.

CONCLUSION REMARKS

Non-alcoholic steatohepatitis (NASH) is one of the most common forms of liver disease encountered in Western society. The present study is the first to evaluate the effects of T3 and GC-1, a TRβ-selective agonist, on fatty liver and steatohepatitis induced in rats fed a choline-deficient, methionine-restricted (CMD) diet. This model results in changes in the liver similar to those observed in human NASH.

Viewed together, we observed that triiodothyronine exerts a strong inhibitory effect on the development of steatosis. Moreover, we found that the vastly increased expression of genes involved in peroxisomal and mitochondrial β-oxidation, as well as a decrease in the protein expression of L-FABP most likely account for reduced hepatic triglyceride content and prevention of hepatic steatosis. T3 also caused a rapid regression of fully established steatosis. This view was strengthened by dramatically reduced expression of COX-2, down-regulation of phospho-STAT 3 and JNK pathways, usually activated in inflammatory processes, as well as accompanied by a significant reduction of serum transaminases. We also noted that GC-1, a synthetic analog of thyroid hormone, selective for both binding and activation functions of TRβ1 over TRα1, shares the capability of T3 to prevent and reverse steatosis. Devoid of thyrotoxic effects, GC-1 represents potentially valuable therapeutic advance as an agent for the treatment of liver damage with the possible relevance of the results of this study to humans.

The initial results obtained with UPLC-QTOF-MS showed that this highly sensitive technique facilitates the achievement of an accurate picture of the changes in the liver lipid profile with relevance to the future studies in identifying specific changes in lipid composition at very early stages of hepatic steatosis using the plasma. The metabolomic approach could also lead to the development of non-invasive techniques in order to replace liver biopsy.

REFERENCES

REFERENCES

Adams LA, Angulo P. Recent concepts in non-alcoholic fatty liver disease. Diabet Med 2005;22(9):1129-33

Adams LA, Angulo P, Lindor KD. Nonalcoholic fatty liver disease. CMAJ 2005;172(7):899-905

Anderson N, Borlak J. Molecular mechanisms and therapeutic targets in steatosis and steatohepatitis. Pharmacol Rev 2008;60(3):311-57

Aranda A, Pascual A. Nuclear hormone receptors and gene expression. Physiol Rev 2001;81(3):1269-304

Baskin-Bey ES, Anan A, Isomoto H, Bronk SF, Gores GJ. Constitutive androstane receptor agonist, TCPOBOP, attenuates steatohepatitis in the methionine choline deficient diet-fed mouse. World J Gastroenterol 2007;13(42):5635-41

Bassett JH, Harvey CB, Williams GR. Mechanisms of thyroid hormone receptor-specific nuclear and extra nuclear actions. Mol Cell Endocrinol 2003;213(1):1-11

Beattie I, Joncour K, Lawson K. Ultra Performance Liquid Chromatography Coupled to Orthogonal Quadrupole TOF-MS(MS) for Metabolite Identification. [Online] [2005] Available from: URL:http://chromatographyonline.findpharma.com/lcgc/data/articlestandard/lcgc/242005/164649/article.pdf

Begriche K, Igoudjil A, Pessayre D, Fromenty B. Mitochondrial dysfunction in NASH: causes, consequences and possible means to prevent it. Mitochondrion 2006;6(1):1-28

Belfort R, Harrison SA, Brown K, Darland C, Finch J, Hardies J, Balas B, Gastaldelli A, Tio F, Pulcini J, Berria R, Ma JZ, Dwivedi S, Havranek R, Fincke C, DeFronzo R, Bannayan GA, Schenker S, Cusi K. A placebo-controlled trial of pioglitazone in subjects with nonalcoholic steatohepatitis. N Engl J Med 2006;30;355(22):2297-307

Bleicher L, Aparicio R, Nunes FM, Martinez L, Gomes Dias SM, Figueira AC, Santos MA, Venturelli WH, da Silva R, Donate PM, Neves FA, Simeoni LA, Baxter JD, Webb P, Skaf MS, Polikarpov I. Structural basis of GC-1 selectivity for thyroid hormone receptor isoforms. BMC Struct Biol 2008;31;8:8

Bradbury MW. Lipid metabolism and liver inflammation. I. Hepatic fatty acid uptake: possible role in steatosis. Am J Physiol Gastrointest Liver Physiol 2006;290(2):G194-8

Browning JD, Horton JD. Molecular mediators of hepatic steatosis and liver injury. J Clin Invest 2004;114(2):147-52

Brunt EM, Janney CG, Di Bisceglie AM, Neuschwander-Tetri BA, Bacon BR. Nonalcoholic steatohepatitis: a proposal for grading and staging the histological lesions. Am J Gastroenterol 1999;94(9):2467-74

Castellan LW, Wilcox HC, Heimberg M. Relationships between fatty acid synthesis and lipid secretion in the isolated perfused rat liver: effects of hyperthyroidism, glucose and oleate. Biochim Biophys Acta 1991;1086(2):197-208

Chandar N, Lombardi B. Liver cell proliferation and incidence of hepatocellular carcinomas in rats fed consecutively a choline-devoid and a choline-supplemented diet. Carcinogenesis 1988;9(2):259-63

Chiellini G, Apriletti JW, Yoshihara HA, Baxter JD, Ribeiro RCJ, Scanlan TS. A high affinity subtype-selective agonist ligand for the thyroid hormone receptor. Chem Biol 1998;5:299-306

Chmurzyńska A. The multigene family of fatty acid-binding proteins (FABPs): function, structure and polymorphism. J Appl Genet 2006;47(1):39-48

Choi SS, Diehl AM. Hepatic triglyceride synthesis and nonalcoholic fatty liver disease. Curr Opin Lipidol 2008;19(3):295-300

Clarke CJ, Haselden JN. Metabolic profiling as a tool for understanding mechanisms of toxicity. Toxicol Pathol 2008;36(1):140-7

Cooke MS, Evans MD, Dizdaroglu M, Lunec J. Oxidative DNA damage: mechanisms, mutation, and disease. FASEB J 2003;17(10):1195-214

Darnell JE Jr, Kerr IM, Stark GR. Jak-STAT pathways and transcriptional activation in response to IFNs and other extracellular signaling proteins. Science 1994;264(5164):1415-21

Das K, Kar P. Non-alcoholic steatohepatitis. J Assoc Physicians India 2005;53:195-9

Day CP, James OF. Steatohepatitis: a tale of two hits? Gastroenterology 1998;114(4):842-5

den Boer M, Voshol PJ, Kuipers F, Havekes LM, Romijn JA. Hepatic steatosis: a mediator of the metabolic syndrome. Lessons from animal models. Arterioscler Thromb Vasc Biol 2004;24(4):644-9

Diehl AM, Li ZP, Lin HZ, Yang SQ. Cytokines and the pathogenesis of non-alcoholic steatohepatitis. Gut 2005;54(2):303-6

Esterbauer H, Cheeseman KH. Determination of aldehydic lipid peroxidation products: Malonaldehyde and 4-hydroxynonenal. Meth Enzymol 1990;186,407-421

Esterbauer H, Schaur RJ, Zollner H. Chemistry and Biochemistry of 4-Hydroxynonenal, Malonaldehyde and Related Aldehydes. Free Radic Biol Med 1991;11(1):81-128

Fahy E, Subramaniam S, Brown HA, Glass CK, Merrill AH Jr, Murphy RC, Raetz CR, Russell DW, Seyama Y, Shaw W, Shimizu T, Spener F, van Meer G, VanNieuwenhze MS, White SH, Witztum JL, Dennis EA. A comprehensive classification system for lipids. J Lipid Res 2005;46(5):839-61

Fan C-Y, Pan J, Usuda N, Yeldandi AV, Rao MS, Reddy JK. Steatohepatitis, spontaneous peroxisome proliferation and liver tumors in mice lacking peroxisomal fatty acyl-CoA oxidase. J Biol Chem 1998;273(25):15639-45

Farrell GC, Larter CZ. Nonalcoholic fatty liver disease: from steatosis to cirrhosis. Hepatology 2006;43(2 Suppl 1):S99-S112

Fishman S, Muzumdar RH, Atzmon G, Ma X, Yang X, Einstein FH, Barzilai N. Resistance to leptin action is the major determinant of hepatic triglyceride accumulation in vivo. FASEB J 2007;21(1):53-60

Furuhashi M, Hotamisligil GS. Fatty acid-binding proteins: role in metabolic diseases and potential as drug targets. Nat Rev Drug Discov 2008;7(6):489-503

Gao B. Cytokines, STATs and liver disease. Cell Mol Immunol 2005;2(2):92-100

George J, Liddle C. Nonalcoholic fatty liver disease: pathogenesis and potential for nuclear receptors as therapeutic targets. Mol Pharm 2007;5(1):49-59

Gérard-Monnier D, Erdelmeier I, Régnard K, Moze-Henry N, Yadan JC, Chaudière J. Reactions of 1-methyl-2-phenylindole with malondialdehyde and 4-hydroxyalkenals. Analytical applications to a colorimetric assay of lipid peroxidation. Chem Res Toxicol 1998;11(10):1176-83

Germain P, Staels B, Dacquet C, Spedding M, Laudet V. Overview of nomenclature of nuclear receptors. Pharmacol Rev 2006;58(4):685-704

Ghoshal AK, Farber E. The induction of liver cancer by dietary deficiency of choline and methionine without added carcinogens. Carcinogenesis 1984;5(10):1367-70

Ghoshal AK, Rushmore TH, Farber E. Initiation of carcinogenesis by a dietary deficiency of choline in the absence of added carcinogens. Cancer Lett 1987;36(3):289-96

Griffin JL. Understanding mouse models of disease through metabolomics. Curr Opin Chem Biol 2006;10(4):309-15

Griffin JL. The Cinderella story of metabolic profiling: does metabolomics get to go to the functional genomics ball? Philos Trans R Soc Lond B Biol Sci 2006;29;361(1465):147-61

Grover GJ, Egan DM, Sleph PG, Beehler BC, Chiellini G, Nguyen NH, Baxter JD, Scanlan TS. Effects of the thyroid hormone receptor agonist GC-1 on metabolic rate and cholesterol in rats and primates: selective actions relative to 3,5,3'-triiodo-L-thyronine. Endocrinology 2004;145(4):1656-61

Halliwell B, Chirico S. Lipid peroxidation: its mechanism, measurement, and significance. Am J Clin Nutr 1993;57(suppl):715S-25S

Han X, Sosnowska D, Bonkowski EL, Denson LA. Growth hormone inhibits signal transducer and activator of transcription 3 activation and reduces disease activity in murine colitis. Gastroenterology 2005;129(1):185-203

Harvey CB, Bassett JH, Maruvada P, Yen PM, Williams GR. The rat thyroid hormone receptor (TR) Deltabeta3 displays cell-, TR isoform-, and thyroid hormone response element-specific actions. Endocrinology 2007;148(4):1764-73

Hensley K, Kotake Y, Sang H, Pye QN, Wallis GL, Kolker LM, Tabatabaie T, Stewart CA, Konishi Y, Nakae D, Floyd RA. Dietary choline restriction causes complex I dysfunction and increased H(2)O(2) generation in liver mitochondria. Carcinogenesis 2000;21(5):983-9

Higgins GM, Anderson RM. Experimental pathology of the liver. I. Restoration of the liver of the while rat following partial surgical removal. Archives of Pathology and Laboratory Medicine 1931;12:186-202

Hinz B, Brune K. Cyclooxygenase-2—10 years later. J Pharmacol Exp Ther 2002;300(2):367-75

Hulbert AJ. Thyroid hormones and their effects: a new perspective. Biol Rev 2000;75(4):519-631

Ibdah JA, Paul H, Zhao Y, Binford S, Salleng K, Cline M, Matern D, Bennett MJ, Rinaldo P, Strauss AW. Lack of mitochondrial trifunctional protein in mice causes neonatal hypoglycemia and sudden death. J Clin Invest 2001;107(11):1403-9

Ip E, Farrell GC, Robertson G, Hall P, Kirsch R, Leclercq I. Central role of PPARalpha-dependent hepatic lipid turnover in dietary steatohepatitis in mice. Hepatology 2003;38(1):123-32

Ip E, Farrell GC, Hall P, Robertson G, Leclercq I. Administration of the potent PPARα agonist Wy-14,643, reverses nutritional fibrosis and steatohepatitis in mice. Hepatology 2004;39(5):1286-96

Janero DR. Malondialdehyde and thiobarbituric acid-reactivity as diagnostic indices of lipid peroxidation and peroxidative tissue injury. Free Radic Biol Med 1990;9(6):515-40

Jansen MS, Cook GA, Song S, Park EA. Thyroid hormone regulates carnitine palmitoyltransferase Iα gene expression through elements in the promoter and first intron. J Biol Chem 2000;275(45):34989-97

Jiang J, Torok N. Nonalcoholic steatohepatitis and the metabolic syndrome. Metab Syndr Relat Disord 2008;6(1):1-7

Johansson L, Rudling M, Scanlan TS, Lundasen T, Webb P, Baxter J, Angelin B, Parini P. Selective thyroid receptor modulation by GC-1 reduces serum lipids and stimulates steps of reverse cholesterol transport in euthyroid mice. Proc Natl Acad Sci USA 2005;102(29):10297-302

Johnson GL, Nakamura K. The c-jun kinase/stress-activated pathway: regulation, function and role in human disease. Biochim Biophys Acta 2007;1773(8):1341-8

Jump DB, Botolin D, Wang Y, Xu J, Christian B, Demeure O. Fatty acid regulation of hepatic gene transcription. J Nutr 2005;135(11):2503-6

Kashireddy PV, Rao MS. Lack of peroxisome proliferator-activated receptor alpha in mice enhances methionine and choline deficient diet-induced steatohepatitis. Hepatol Res 2004;30(2):104-110

Kashireddy PR, Rao MS. Sex differences in choline-deficient diet-induced steatohepatitis in mice. Exp Biol Med (Maywood) 2004;229(2):158-62

Kass GE. Mitochondrial involvement in drug-induced hepatic injury. Chem Biol Interact 2006;163(1-2):145-59

Kirsch R, Clarkson V, Shephard EG, Marais DA, Jaffer MA, Woodburne VE, Kirsch RE, Hall Pde L. Rodent nutritional model of non-alcoholic steatohepatitis: species, strain and sex difference studies. J Gastroenterol Hepatol 2003;18(11):1272-82

Koteish A, Diehl AM. Animal models of steatohepatitis. Best Pract Res Clin Gastroenterol 2002;16(5):679-90

Kumagai T, Kawamoto Y, Nakamura Y, Hatayama I, Satoh K, Osawa T, Uchida K. 4-hydroxy-2-nonenal, the end product of lipid peroxidation, is a specific inducer of cyclooxygenase-2 gene expression. Biochem Biophys Res Commun 2000;273(2):437-41

Lanni A, Moreno M, Lombardi A, de Lange P, Silvestri E, Ragni M, Farina P, Baccari GC, Fallahi P, Antonelli A, Goglia F. 3,5-Diiodo-L-thyronine powerfully reduces adiposity in rats by increasing the burning of fats. FASEB J 2005;19(11):1552-4

Laurin J, Lindor KD, Crippin JS, Gossard A, Gores GJ, Ludwig J, Rakela J, McGill DB. Ursodeoxycholic acid or clofibrate in the treatment of non-alcohol-induced steatohepatitis: a pilot study. Hepatology 1996;23(6):1464-7

Lazar MA. Thyroid hormone receptors: multiple forms, multiple possibilities. Endocr Rev 1993;14(2):184-93

Lazar MA. Thyroid hormone action: a binding contract. J Clin Invest 2003;112(4):497-9

Leclercq IA, Farrell GC, Sempoux C, dela Peña A, Horsmans Y. Curcumin inhibits NF-kappaB activation and reduces the severity of experimental steatohepatitis in mice. J Hepatol 2004;41(6):926-34

Ledda-Columbano GM, Pibiri M, Concas D, Molotzu F, Simula G, Cossu C, Columbano A. Sex difference in the proliferative response of mouse hepatocytes to treatment with the CAR ligand, TCPOBOP. Carcinogenesis 2003;24(6):1059-65

Lefebvre P, Chinetti G, Fruchart JC, Staels B. Sorting out the roles of PPAR alpha in energy metabolism and vascular homeostasis. J Clin Invest 2006;116(3):571-80

Levy DE, Lee CK. What does Stat3 do? J Clin Invest 2002;109(9):1143-8

Li Z, Vance DE. Thematic Review Series: Glycerolipids. Phosphatidylcholine and choline homeostasis. J Lipid Res 2008; 49(6):1187-94

Linden D, Alsterholm M, Wennbo H, Oscarsson J. PPARalpha deficiency increases secretion and serum levels of apolipoprotein B-containing lipoproteins. Lipid Res 2001;42(11):1831-40

Liu H, Jones BE, Bradham C, Czaja MJ. Increased cytochrome P-450 2E1 expression sensitises hepatocytes to c-jun mediated cell death from TNF-alpha. Am J Physiol Gastrointest Liver Physiol 2002;282(2):G257-66

Lombardi B, Pani P, Schlunk FF. Choline-deficiency fatty liver: impaired release of hepatic triglycerides. J Lipid Res 1968;9(4):437-46

Lovato P, Brender C, Agnholt J, Kelsen J, Kaltoft K, Svejgaard A, Eriksen KW, Woetmann A, Ødum N. Constitutive STAT3 activation in intestinal T cells from patients with Crohn's disease. J Biol Chem 2003;278(19):16777-81

Lu SC, Alvarez L, Huang ZZ, Chen L, An W, Corrales FJ, Avila MA, Kanel G, Mato JM. Methionine adenosyltransferase 1A knockout mice are predisposed to liver injury and exhibit increased expression of genes involved in proliferation. Proc Natl Acad Sci USA 2001;98(10):5560-5

Marra F, Efsen E, Romanelli RG, Caligiuri A, Pastacaldi S, Batignani G, Bonacchi A, Caporale R, Laffi G, Pinzani M, Gentilini P. Ligands of peroxisome proliferator-activated receptor gamma modulate profibrogenic and proinflammatory actions in hepatic stellate cells. Gastroenterology 2000;119(2):466-78

Mattila I, Seppänen-Laakso T, Suortti T, Oresic M. Application of lipidomics and metabolomics to the study of adipose tissue. Methods Mol Biol 2008;456:123-30

Michel V, Yuan Z, Ramsubir S, Bakovic M. Choline transport for phospholipid synthesis. Exp Biol Med (Maywood) 2006;231(5):490-504

Minden A, Karin M. Regulation and function of the JNK subgroup of MAP kinases. Biochim Biophys Acta 1997;1333(2):F85-104

Miyazaki Y, Mahankali A, Matsuda M, Mahankali S, Hardies J, Cusi K, Mandarino LJ, DeFronzo RA. Effect of pioglitazone on abdominal fat distribution and insulin sensitivity in type 2 diabetic patients. J Clin Endocrinol Metab 2002;87(6):2784-91

Moitra J, Mason MM, Olive M, Krylov D, Gavrilova O, Marcus-Samuels B, Feigenbaum L, Lee E, Aoyama T, Eckhaus M, Reitman ML, Vinson C. Life without white fat: a transgenic mouse. Genes Dev 1998;12(20):3168-81

Moreno M, de Lange P, Lombardi A, Silvestri E, Lanni A, Goglia F. Metabolic effects of thyroid hormone derivatives. Thyroid 2008;18(2):239-53

Mudter J, Weigmann B, Bartsch B, Kiesslich R, Strand D, Galle PR, Lehr HA, Schmidt J, Neurath MF. Activation pattern of signal transducers and activators of transcription (STAT) factors in inflammatory bowel diseases. Am J Gastroenterol 2005;100, 64-72

Nagasawa T, Inada Y, Nakano S, Tamura T, Takahashi T, Maruyama K, Yamazaki Y, Kuroda J, Shibata N. Effects of bezafibrate, PPAR pan-agonist, and GW501516, PPARδ agonist, on development of steatohepatitis in mice fed a methionine- and choline-deficient diet. Eur J Pharmacol 2006;536(1-2):182-91

Nakatani Y, Kaneto H, Kawamori D, Hatazaki M, Miyatsuka T, Matsuoka TA, Kajimoto Y, Matsuhisa M, Yamasaki Y, Mori M. Modulation of the JNK pathway in liver affects insulin resistance status. J Biol Chem 2004;279(44):45803-9

Newberry EP, Xie Y, Kennedy S, Han X, Buhman KK, Luo J, Gross RW, Davidson NO. Decreased hepatic triglyceride accumulation and altered fatty acid uptake in mice with deletion of the liver fatty acid-binding protein gene. J Biol Chem 2003;278(51):51664-72

Newberry EP, Xie Y, Kennedy SM, Luo J, Davidson NO. Protection against Western diet-induced obesity and hepatic steatosis in liver fatty acid-binding protein knockout mice. Hepatology 2006;44(5):1191-205

Neuschwander-Tetri BA, Brunt EM, Wehmeier KR, Oliver D, Bacon BR. Improved nonalcoholic steatohepatitis after 48 weeks of treatment with the PPAR-gamma ligand rosiglitazone. Hepatology 2003;38(4):1008-17

Neuschwander-Tetri BA, Caldwell SH. Nonalcoholic steatohepatitis: summary of an AASLD Single Topic Conference. Hepatology 2003;37(5):1202-19

Nguyen P, Leray V, Diez M, Serisier S, Le Bloc'h J, Siliart B, Dumon H. Liver lipid metabolism. J Anim Physiol Anim Nutr (Berl) 2008;92(3):272-83

Nicholson JK, Lindon JC, Holmes E. 'Metabonomics': understanding the metabolic responses of living systems to pathophysiological stimuli via multivariate statistical analysis of biological NMR spectroscopic data. Xenobiotica 1999;29(11):1181-9

Norris AW, Spector AA. Very long chain n-3 and n-6 polyunsaturated fatty acids bind strongly to liver fatty acid-binding protein. J Lipid Res 2002;43(4):646-53

Oetting A, Yen PM. New insights into thyroid hormone action. Best Pract Res Clin Endocrinol Metab 2007;21(2):193-208

Oldiges M, Lütz S, Pflug S, Schroer K, Stein N, Wiendahl C. Metabolomics: current state and evolving methodologies and tools. Appl Microbiol Biotechnol 2007;76(3):495-511

Ota T, Takamura T, Kurita S, Matsuzawa N, Kita Y, Uno M, Akahori H, Misu H, Sakurai M, Zen Y, Nakanuma Y, Kaneko S. Insulin resistance accelerates a dietary rat model of nonalcoholic steatohepatitis. Gastroenterology 2007;132(1):282-93

Pibiri M, Ledda-Columbano GM, Cossu C, Simbula G, Menegazzi M, Shinozuka H, Columbano A. Cyclin D1 is an early target in hepatocyte proliferation induced by thyroid hormone (T3). FASEB J 2001;15(6):1006-13

Plumb RS, Stumpf CL, Granger JH, Castro-Perez J, Haselden JN, Dear GJ. Use of liquid chromatography/time-of-flight mass spectrometry and multivariate statistical analysis shows promise for the detection of drug metabolites in biological fluids. Rapid Commun Mass Spectrom 2003;17(23):2632-8

Ramaiah SK. A toxicologist guide to the diagnostic interpretation of hepatic biochemical parameters. Food Chem Toxicol 2007;45(9):1551-7

Rao MS, Papreddy JK, Musunuri S, Okonkwo A. Prevention/reversal of choline deficiency-induced steatohepatitis by a peroxisome proliferators-activated receptor alpha ligand in rats. In Vivo 2002;16(2):145-52

Reddy JK. Nonalcoholic steatosis and steatohepatitis. III Peroxisomal β-oxidation, PPARα, and steatohepatitis. Am J Physiol Gastrointest Liver Physiol 2001;281(6):G1333-9

Reddy JK, Hashimoto T. Peroxisomal beta-oxidation and peroxisome proliferator-activated receptor alpha: an adaptive metabolic system. Annu Rev Nutr 2001;21:193-230

Reddy JK, Rao MS. Lipid metabolism and liver inflammation. II. Fatty liver disease and fatty acid oxidation. Am J Physiol Gastrointest Liver Physiol 2006;290(5):G852-8

Ribeiro MO. Effects of thyroid hormone analogs on lipid metabolism and thermogenesis. Thyroid 2008;18(2):197-203

Rinella ME, Elias MS, Smolak RR, Fu T, Borensztajn J, Green RM. Mechanisms of hepatic steatosis in mice fed a lipogenic methionine choline-deficient diet. J Lipid Res 2008;49(5):1068-76

Roberts LD, McCombie G, Titman CM, Griffin JL. A matter of fat: An introduction to lipidomic profiling methods. J Chromatogr B Analyt Technol Biomed Life Sci 2008;15;871(2):174-81

Robertson G, Leclercq I, Farrell GC. Nonalcoholic steatosis and steatohepatitis. II. Cytochrome P-450 enzymes and oxidative stress. Am J Physiol Gastrointest Liver Physiol 2001;281(5):G1135-9

Romestaing C, Piquet MA, Bedu E, Rouleau V, Dautresme M, Hourmand-Ollivier I, Filippi C, Duchamp C, Sibille B. Long term highly saturated fat diet does not induce NASH in Wistar rats. Nutr Metab (Lond) 2007;21;4:4

Rushmore TH, Lim YP, Farber E, Ghoshal AK. Rapid lipid peroxidation in the nuclear fraction of rat liver induced by a diet deficient in choline and methionine. Cancer Lett 1984;24(3):251-5

Rushmore TH, Farber E, Ghoshal AK, Parodi S, Pala M, Taningher M. A choline-devoid diet, carcinogenic in the rat, induces DNA damage and repair. Carcinogenesis 1986;7(10):1677-80

Sanyal AJ, Mofrad PS, Contos MJ, Sargeant C, Luketic VA, Sterling RK, Stravitz RT, Shiffman ML, Clore J, Mills AS. A pilot study of vitamin E versus vitamin E and pioglitazone for the treatment of nonalcoholic steatohepatitis. Clin Gastroenterol Hepatol 2004;2(12):1107-15

Sap J, Muñoz A, Damm K, Goldberg Y, Ghysdael J, Leutz A, Beug H, Vennström B. The c-erb-A protein is a high-affinity receptor for thyroid hormone. Nature 1986;324(6098):635-40

Sawada N, Poirier L, Moran S, Xu YH, Pitot HC. The effect of choline and methionine deficiencies on the number and volume percentage of altered hepatic foci in the presence or absence of diethylnitrosamine initiation in rat liver. Carcinogenesis 1990;11(2):273-81

Schattenberg JM, Singh R, Wang Y, Lefkowitch JH, Rigoli RM, Scherer PE, Czaja MJ. JNK1 but not JNK2 promotes the development of steatohepatitis in mice. Hepatology 2006;43(1):163-72

Schreuder TC, Verwer BJ, van Nieuwkerk CM, Mulder CJ. Nonalcoholic fatty liver disease: An overview of current insights in pathogenesis, diagnosis and treatment. World J Gastroenterol 2008;14(16):2474-86

Schroeder-Gloeckler JM, Rahman SM, Janssen RC, Qiao L, Shao J, Roper M, Fischer SJ, Lowe E, Orlicky DJ, McManaman JL, Palmer C, Gitomer WL, Huang W, O'Doherty RM, Becker TC, Klemm DJ, Jensen DR, Pulawa LK, Eckel RH, Friedman JE. CCAAT/ enhancer-binding protein beta deletion reduces adiposity, hepatic steatosis, and diabetes in Lepr(db/db) mice. J Biol Chem 2007;282(21):15717-29

Seki S, Kitada T, Yamada T, Sakaguchi H, Nakatani K, Wakasa K. In situ detection of lipid peroxidation and oxidative DNA damage in non-alcoholic fatty liver diseases. J Hepatol 2002;37(1):56-62

Serviddio G, Sastre J, Bellanti F, Viña J, Vendemiale G, Altomare E. Mitochondrial involvement in non-alcoholic steatohepatitis. Mol Aspects Med 2007;29(1-2):22-35
Shelness GS, Sellers JA. Very-low-density lipoprotein assembly and secretion. Curr Opin Lipidol 2001;12(2):151-7

Shimano H, Horton JD, Hammer RE, Shimomura I, Brown MS, Goldstein JL. Overproduction of cholesterol and fatty acids causes massive liver enlargement in transgenic mice expressing truncated SREBP-1a. J Clin Invest 1996;98(7):1575-84

Shimano H. Sterol regulatory element-binding proteins (SREBPs): transcriptional regulators of lipid synthetic genes. Prog Lipid Res 2001;40(6):439-52

Shimomura I, Hammer RE, Richardson JA, Ikemoto S, Bashmakov Y, Goldstein JL, Brown MS. Insulin resistance and diabetes mellitus in transgenic mice expressing nuclear SREBP-1c in adipose tissue: model for congenital generalized lipodystrophy. Genes Dev 1998;12(20):3182-94

Shinozuka H, Lombardi B, Sell S, Iammarino RM. Early histological and functional alterations of ethionine liver carcinogenesis in rats fed a choline-deficient diet. Cancer Res 1978;38(4):1092-8

Shinozuka H, Sells MA, Katyal SL, Sell S, Lombardi B. Effects of a choline-devoid diet on the emergence of gamma-glutamyltranspeptidase-positive foci in the liver of carcinogen-treated rats. Cancer Res 1979;39(7 Pt 1):2515-21

Smith CA, Want EJ, O'Maille G, Abagyan R, Siuzdak G. XCMS: processing mass spectrometry data for metabolite profiling using nonlinear peak alignment, matching, and identification. Anal Chem 2006;1;78(3):779-87

Storch J, Thumser AE. The fatty acid transport function of fatty acid-binding proteins. Biochim Biophys Acta 2000;1486(1):28-44

Suzuki A, Hanada T, Mitsuyama K, Yoshida T, Kamizono S, Hoshino T, Kubo M, Yamashita A, Okabe M, Takeda K, Akira S, Matsumoto S, Toyonaga A, Sata M, Yoshimura A. CIS3/SOCS3/SSI3 plays a negative regulatory role in STAT3 activation and intestinal inflammation. J Exp Med 2001;193(4):471-81

Swartz ME. Ultra Performance Liquid Chromatography (UPLC): An Introduction. [Online] [2005] Available from: URL:http://chromatographyonline.findpharma.com/lcgc/data/articlestandard//lcgc/242005/164646/article.pdf

Thompson J, Reese-Wagoner A, Banaszak L. Liver fatty acid binding protein: species variation and the accommodation of different ligands. Biochim Biophys Acta 1999;1441(2-3):117-30

Tobin JF, Freedman LP. Nuclear receptors as drug targets in metabolic diseases: new approaches to therapy. Trends Endocrinol Metab 2006;17(7):284-90

Trost SU, Swanson E, Gloss B, Wang-Iverson DB, Zhang H, Volodarsky T, Grover GJ, Baxter JD, Chiellini G, Scanlan TS, Dillmann WH. The Thyroid Hormone Receptor-β-Selective Agonist GC-1 Differentially Affects Plasma Lipids and Cardiac Activity. Endocrinology 2000;141(9):3057-64

Turkson J, Jove R. STAT proteins: novel molecular targets for cancer drug discovery. Oncogene 2000;19(56):6613-26

Vendemiale G, Grattagliano I, Altomare E, Serviddio G, Portincasa P, Prigigallo F, Palasciano G. Mitochondrial oxidative damage and myocardial fibrosis in rats chronically intoxicated with moderate doses of ethanol. Toxicol Lett 2001;123(2-3):209-16

Veteläinen R, van Vliet A, van Gulik TM. Essential pathogenic and metabolic differences in steatosis induced by choline or methione-choline deficient diets in a rat model. J Gastroenterol Hepatol 2007;22(9):1526-33

Villas-Bôas SG, Mas S, Akesson M, Smedsgaard J, Nielsen J. Mass spectrometry in metabolome analysis. Mass Spectrom Rev 2005;24(5):613-46

Villicev CM, Freitas FRS, Aoki MS, Taffarel C, Scanlan TS, Moriscot AS, Ribeiro MO, Bianco AC, Gouveia CHA. Thyroid hormone receptor b-specific agonist GC-1 increases energy expenditure and prevents fat-mass accumulation in rats. J Endocrinol 2007;193(1):21-9

Wanders RJA. Peroxisomes, lipid metabolism, and peroxisomal disorders. Mol Genet Metab 2004;83(1-2):16-27

Weinberger C, Thompson CC, Ong ES, Lebo R, Gruol DJ, Evans RM. The c-erb-A gene encodes a thyroid hormone receptor. Nature 1986;324(6098):641-6

Weltman MD, Farrell GC, Hall P, Ingelman-Sundberg M, Liddle C. Hepatic cytochrome P450 2E1 is increased in patients with nonalcoholic steatohepatitis. Hepatology 1998;27(1):128-33

Williams GR. Cloning and characterization of two novel thyroid hormone receptor beta isoforms. Mol Cell Biol 2000;20(22):8329-42

Xie GX, Ni Y, Su MM, Zhang YY, Zhao AH, Gao XF, Liu Z, Xiao PG, Jia W. Application of ultra-performance LC-TOF MS metabolite profiling techniques to the analysis of medicinal Panax herbs. Metabolomics 2008;4:248-260

Yao ZM, Vance DE. The active synthesis of phosphatidylcholine is required for very low density lipoprotein secretion from rat hepatocytes. J Biol Chem 1988;263(6):2998-3004

Yen PM. Physiological and molecular basis of thyroid hormone action. Physiol Rev 2001;81(3):1097-142

Yetukuri L, Katajamaa M, Medina-Gomez G, Seppänen-Laakso T, Vidal-Puig A, Oresic M. Bioinformatics strategies for lipidomics analysis: characterization of obesity related hepatic steatosis. BMC Syst Biol 2007;15;1:12

Yokoyama S, Sells MA, Reddy TV, Lombardi B. Hepatocarcinogenic and promoting action of a choline-devoid diet in the rat. Cancer Res 1985;45(6):2834-42

Yoshiji H, Nakae D, Mizumoto Y, Horiguchi K, Tamura K, Denda A, Tsujii T, Konishi Y. Inhibitory effect of dietary iron deficiency on inductions of putative preneoplastic lesions as well as 8-hydroxydeoxyguanosine in DNA and lipid peroxidation in the livers of rats caused by exposure to a choline-deficient L-amino acid defined diet. Carcinogenesis 1992;13(7):1227-33

Yu J, Ip E, Dela Pena A, Hou JY, Sesha J, Pera N, Hall N, Kirsch R, Leclercq I, Farrell GC. COX-2 induction in mice with experimental nutritional steatohepatitis: role as pro-inflammatory mediator. Hepatology 2006;43(4):826-36

Zeisel SH. Choline deficiency. J Nutr Biochem 1990;1(7):332-49

Zeisel SH. Choline: an essential nutrient for humans. Nutrition 2000;16(7-8):669-71

Zeisel SH. Choline: critical role during fetal development and dietary requirements in adults. Annu Rev Nutr 2006;26:229-50